USING PXRF AND ICP-MS ANALYSES TO CREATE A CALIBRATION CURVE FOR SILICIFIED SANDSTONES IN THE UPPER MISSISSIPPI RIVER VALLEY (UMRV)

By:

Taylor Roessler

Submitted to the Faculty of

The Archaeology Studies Program

Department of Archaeology and Anthropology

In partial fulfillment for the requirements for the degree of

Bachelor of Sciences

University of Wisconsin-La Crosse

2016

USING PXRF AND ICP-MS ANALYSES TO CREATE A CALIBRATION AND QUANTIFICATION STANDARDS FOR THREE SILICIFIED SANDSTONES IN THE UPPER MISSISSIPPI RIVER VALLEY (UMRV)

Taylor Roessler B.S.

University of Wisconsin La-Crosse 2016

ABSTRACT

Silicified sandstones are commonly found in lithic assemblages at sites in, and around, the Upper Mississippi River Valley (UMRV). This study resulted in compositionally characterizing three silicified sandstones (Arcadia Ridge, Cataract, and Hixton) and created calibration and quantification standards for raw pXRF data using ICP-MS data as my known. My results indicate that pXRF analysis, coupled with quantification and calibration standards from ICP-MS analysis, can be conducted reliably on heterogeneous materials like silicified sandstones, to varying degrees dependent on the element being analyzed. In addition I found that these three silicified sandstones can be differentiated at the geologic formation, by using analysis of concentrations of several elements. The results of this study will allow for the non-destructive geochemical sourcing of these materials, to the formation level, using pXRF analysis alone. Upon determining lithic resource procurement strategies at sites, human behaviors can be examined by looking at the relationship between the lithic material utilized and the distance of the site from the source. These behaviors include, population movements, landscape patterning, and trade or exchange networks.

ACKNOWLEDGEMETS

First I would like to thank all of my professors throughout my college career; their hard work provided me with the proper knowledge base to pursue fields of study that interest me. I would like to give a special thanks to George Christiansen III and Constance Arzigian; these individuals provided an immeasurable amount of guidance and knowledge throughout my academic career. I would like to thank Jessi Halligan, who not only served as my reader but has provided me multiple opportunities to pursue various research interest, and has assisted me with this project from its beginning. I would also like to thank Robert "Ernie" Boszhardt, whose past research made this study possible, but has also provided me with resources, practical skills, and direction, all of which made this study possible today. I would also like to thank Heather Walder, who not only served as my instructor but also provided feedback and numerous resources.

A special thanks to the Under-Graduate Research and Grant Committee, who awarded me a grant making the sampling and ICP-MS analysis to this study possible. And a very special thanks to the Geography department at the University of Wisconsin- La Crosse who allowed me to use their pXRF. Also I would like to thank Dr. Colin Belby who provided numerous hours of his own time to help me receive this grant, develop this project, and obtain results, without him this study would not have been possible.

I would also like to thank private collectors and organizations who graciously helped me gather data essential to this project. First, Paul Gardner and The Archaeological Conservancy for allowing me to sample Silver Mound in order to gain essential data for this study. Also a special thanks to Dan Wendt who helped me track down a source of Arcadia Ridge silicified sandstone and whom also provided me with guidance and resources at the beginning of this project. And finally Todd Reichart, who through rain and bad weather aided me with him immense local knowledge of archaeological resources in the area in the Cataract area sampling process.

Finally I would like to thank my peer-readers, family, and friends, all of whom supported this project, provided me with feedback and direction, but also kept me grounded throughout this stressful yet rewarding project. In addition, I would like to thank all those who appreciate and work to protect natural and cultural resources here in Wisconsin and elsewhere. Peace, love, and progress forever. Thank you.

INTRODUCTION

Silicified sandstones in the Upper Mississippi River Valley (UMRV) have been proven to be different in elemental composition on the basis of source area (Boszhardt and Carr 2010:10). Studies utilizing portable X-Ray fluorescence (pXRF) analysis in conjunction with inductively coupled plasma mass spectroscopy (ICP-MS) data have proven to be useful and accurate methods of sourcing lithic assemblages in other regions (Golitko et al. 2010:123). Portable XRF is a preferable method of geochemical analysis because pXRF is relatively inexpensive, can be employed in the field, and is non-destructive. This study gathered pXRF and ICP-MS data on three silicified sandstones; Arcadia Ridge, Cataract, and Hixton that are found in the UMRV. Then, a sample of ICP-MS data was used in an S1 pXRF calibration program to develop calibration and quantification standards for raw pXRF spectra. The calibration and quantification of raw pXRF data allows for easier analysis and comparison of results. First, determined the reliability of pXRF techniques of analysis against ICP-MS analysis, which is more reliable. This study found that pXRF analysis, coupled with quantification and calibration standards from ICP-MS analysis, can be conducted on heterogeneous materials like silicified sandstones, to varying degrees dependent on the element being analyzed. Calibrated pXRF scans show that four elements: nickel, lead, chromium, and zinc are useful in differentiating between Arcadia Ridge, Cataract, and Hixton silicified sandstone; although to varying degrees and at different geologic levels (formation or source level).

Figure 1: Location of sources analyzed. (Google Earth 2016)

Calibration and quantification standards gained from this study, along with elemental ranges established for these sources can then be used in future sourcing studies wishing to determine the source of silicified sandstones found at archaeological sites. The accurate sourcing of silicified sandstones using calibrated, quantified pXRF data will then be possible at archaeological sites around and outside the UMRV. This will be useful because lithic procurement patterns and behaviors can then be discerned based on context of artifact analyzed and the geographic location from which it was derived. This method of analysis can then lead to the discussion of social behaviors such as population movements or trade networks which are two important themes in lithic sourcing studies in the region (Boszhardt and Carr 2010:10). Thus, the

development of a calibration and quantification standards for pXRF data for three commonly occurring silicified sandstones will allow archaeologist to gather pXRF data from silicified sandstones at sites, calibrate and quantify that data using standards established from this study. Then calibrated pXRF data can be compared to known elemental ranges for these source to determine the probable source of lithic materials found at sites. This information will allow researchers utilizing this method to make inferences about specific human behaviors, based on the context of the finds and their relation to the source of the material.

Silicified Sandstones

Silicified Sandstones, or orthoquartzites, are a commonly-occurring lithic material in prehistoric assemblages in the UMRV (Boszhardt 1998). Silicified sandstones occur in outcrops of varying sizes throughout western Wisconsin, and parts of eastern Minnesota (Boszhardt 1998, 2012; Mossler 2008:26, 33; Ostrum 1973; Runkel 2012). The processes leading to the formation of silicified sandstones caused sand grains to become tightly bound in a silica-matrix. High silica content is an attribute of high-quality lithic material for stone tool production (Andrefsky 2005:24). Thus, the high silica content in these sources of silicified sandstone made them a preferable material for stone tool production in the past. Some sources, because of their silica contents and grain sizes were more preferred as "high" quality materials than others. This is apparent when one examines the distribution and context of findings artifacts made of UMRV silicified sandstones. These materials have been found in "high status" contexts such as Mound 72 at Cahokia (Pauketat 2004:121,127), and in surface finds of Paleo-Indian points across the United States (Boszhardt 2003:13-26; Mason 1988:30). This fact, along with the wide distribution of silicified sandstone sources across the western Wisconsin and eastern Minnesota

makes determining the source location of these materials important in order to determine human social behaviors in the past. These social behaviors include the presence of seasonal rounds, logistical movements, and trade networks.

BACKGROUND

Silicified sandstones, in the UMRV were heavily utilized throughout prehistory (Mason 1988:28; Porter 1961). In addition multiple silicified sandstone source occur throughout and around the UMRV (Boszhardt 1998; Boszhardt 2012; Mossler 2008:26,33; Ostrum 1973; Runkel 2012). Because of the prehistoric use of silicified sandstone, and the multiplicity of sources existing in the UMRV, the accurate sourcing of these materials from sites is imperative to being able to draw conclusions about human social behavior based on lithic procurement strategies. I argue that the geochemical sourcing of silicified sandstone artifacts by obtaining calibrated and quantified pXRF data is not only a valid method for the sourcing of silicified sandstones in the UMRV, but that it is preferred because results are backed by quantified, objective data, and also because pXRF is non-destructive and utilizable in the field.

UMRV Silicified Sandstones Geology

Silicified sandstones, sometimes referred to as orthoquartzites form from sandstone being compressed and silicon dioxide permeating through the sandstone binding the grains together tightly in a silica matrix, which allows the stone to break sharply in a controlled manner (Andrefsky 2005:50-53; Ostrum 1973). Wisconsin silicified sandstones formed from the result of Cambrian-aged sandstones absorbing silica from Ordovician-age dolomite deposits which sometimes occur over sandstone deposits. Silica from this limestone permeated through the sandstone, getting caught within the sandstone, binding the sand-grains tightly together in a

silicon-dioxide matrix (Boszhardt 1998:2). Because of this predictability in breaking, silicified sandstones are considered to be fairly high quality stone tool making materials, as long as silica content is high, according to Andrefsky (2005:52-53) and Lang (1987:132).

Several sources of silicified sandstones exist throughout Northwestern Wisconsin and into Eastern Minnesota (Boszhardt 1998; Boszhardt 2012; Mossler 2008:26, 33; Ostrum 1973; Runkel 2012). These deposits of silicified sandstones occur within two geologic formations: the Wonewoc and Jordan Formations. And within these formations exist several regional outcrop sources (Mossler 2008:26-35; Ostrum 1973). Various sources of these silicified sandstones were used throughout prehistory. Extensively utilized prehistoric sources of Wonewoc formation silicified sandstones include Silver Mound, the source of Hixton silicified sandstone (Lang 1987:132; Lang 2004:106) and Cataract silicified sandstone named after its source location (Boszhardt 1998). Extensively utilized Jordan formation silicified sandstone deposits include Arcadia Ridge, the source of Arcadia silicified sandstones, and surrounding outcrops (Boszhardt and Carr 2010:8; Runkel et al. 2012:39). This recognition of various silicified sandstone sources in the UMRV could dramatically change our understanding between people in the past and their relationship to the landscape and their desired source of lithic material.

Pre-Historic Use of Silicified Sandstones

Because of their high silica content, a feature which makes for good "tool-stone" (Andrefsky 2005), silicified sandstones were heavily utilized throughout prehistory. This utilization of silicified sandstone by prehistoric peoples was recognized early in archaeological research of the area (Mason 1988:28; Porter 1961). However, this research was almost exclusively limited to studying and classifying Paleo-Indian points made from silicified sandstones (Mason 1988:28; Hill 1994), or focused on the utilization of Silver Mound, the source

of Hixton silicified sandstone (Boszhardt and Carr 2010:8; Porter 1961). Because of this, many silicified sandstones were assumed to be, or, just referred to as Hixton (Boszhardt 1998:2). The recognition of new sources of prehistorically utilized source of silicified sandstones has implications for of understanding of human pre-history in the UMRV.

Paleo-Indians and Silicified Sandstones

Paleo-Indian studies have a vested interest in silicified sandstone sourcing studies. One attribute of "typical" Paleo-Indian lithic assemblages such as Clovis assemblages is the utilization of high-quality lithic material (Boszhardt 2003:14). Dependent on location, these materials tend to appear in the archaeological record, as artifacts, very far from the original source. This feature of Paleo-Indian lithic assemblages has led many to conclude that either Paleo-Indians were highly mobile people who encountered high quality lithic sources during their seasonal-round, or somehow were able to acquire high-quality material through exchange networks (Mason 1988:25-30). Among many other materials, high-quality silicified sandstones, believed to have originated from Silver Mound, are a fairly abundant and widely distributed material type in Paleo-Indian lithic assemblages (Lang 1987:132; Boszhardt and Carr 2010:19; Mason 1988: 28). Because of the high amount of silicified sandstone in Paleo-Indian lithic assemblages, this material type was immediately recognized as important in North American archaeology and studies immediately began to identify the source of this material type (Boszhardt and Carr 2010:19-21). Because of its unique geography, the density of archaeological resources, and many other factors, Silver Mound was almost immediately inferred to be the likely source of these artifacts (Boszhardt and Carr 2010:5-9). Studies at Silver Mound then tend to focus on identifying activity areas, and determining their cultural affiliation (Hill 1994; Lang 1987). These studies have found that prehistoric use at Silver Mound was extensive during

Paleo-Indian times, and through-out much of Wisconsin pre-history (Boszhardt and Carr 2010; Lang 1987). However, recent findings have called into question the research focus on procurement of silicified sandstone from Silver Mound alone throughout pre-history.

Extensive surveys of Wisconsin's "Orthoquartzite Region" reveled that there are several distinct sources of silicified sandstones, of which, many have been utilized prehistorically. These sources include Cataract, Browns Valley, Arcadia Ridge, and Alma silicified sandstones (Boszhardt 1998). These surveys reveled several "high-quality" sources such as Cataract silicified sandstone and certain Arcadia sources. In addition to that, these surveys were able to attribute Paleo-Indian use to several quarry sites such as Walczak-Wontor pits at Cataract and several localities at Browns Valley (Boszhardt 1998:13-14). These findings may call into question the supposed importance of Silver Mound during Wisconsin prehistory, and especially during Paleo-Indian times (Boszhardt 1998; Boszhardt and Carr 2010). Boszhardt (1998) and Carr (2010:10) have pointed out that geochemical analysis, in the form of sourcing studies could solve this "lack of clarity" in our interpretations of the past, especially concerning population movements, landscape use, territoriality, and alliances and exchange networks (Boszhardt and Carr 2010:24-26). Geochemical sourcing by pXRF offers a reliable means to differentiate between silicified sandstones from archaeological contexts.

Geochemical Sourcing of Silicified Sandstones

Due to geologic conditions and formation processes, silicified sandstones have differing silica contents. This is important because high silica content is directly correlated with high quality of tool, while low silica content is correlated to low quality tool-stone (Andrefsky 2005). In addition silicified sandstone sources have been demonstrated to have differing elemental contents (Boszhardt and Carr 2010), which can affect physical appearance, as well as

"workability" of the material. This variability inherently suggest that certain materials were recognized to be different, preferred, and utilized differently; a statement supported by studies examining selective use of silicified sandstones (Boszhardt and Carr 2010; Carr 2005; Julig et al. 2002). This difference in material preference, use, and/or access at sites can then be analyzed, and potentially explained in terms of human social behavior, dependent on the accurate sourcing of lithic materials from archaeological sites.

Because of the similarity of Arcadia Ridge, Cataract, and Hixton silicified sandstones, along with other silicified sandstone sources (appearance, grain size, structure, etc...), the confident sourcing of silicified sandstones, through macroscopic analysis alone, may be problematic (Boszhardt and Carr 2010:10-11). However, petrographic thin-sectioning, scanning electron microscope (SEM) and several other geochemical techniques including, instrumental neutron activation analysis (INAA), and oxygen isotope analysis have been conducted on Arcadia Ridge, Cataract, and Hixton silicified sandstones (Boszhardt 1998:11-12; Boszhardt and Carr 2010:9-11: Juling et al. 2002). These analyses revealed that each source can be differentiated, albeit to differing degrees, dependent on which method is being used (Boszhardt and Carr 2010:10). Boszhardt and Carr's study, while useful in demonstrating that each source type has its own "elemental signature", utilized mainly destructive means of analysis, with the exception of INAA. However, producing the most accurate INAA results, requires one to homogenize the sample, normally in the form of crushing (Andrefsky 2006:43-45), thereby destroying the artifact. SEM, INAA (where samples are homogenized), Oxygen isotope analysis and petrographic thin-sectioning are types of analysis not conductive to the proper preservation of the archaeological record due to their destructive nature.

Another study, by Juling et al. (2002), aimed at determining the prehistoric use of silicified sandstone resources in the Upper Great Lakes, was also able to differentiate silicified sandstone types using XRF and instrumental neutron activation analysis (INAA). Juling et al.'s (2002) study is important because it demonstrated that non-destructive techniques of analysis can be used to geochemically differentiate silicified sandstone sources that can be found in the UMRV. Once these techniques are refined, the confident geochemical sourcing of silicified sandstones will be possible. Archaeologists could then take silicified sandstone found in archaeological contexts, and apply techniques of geo-chemical analysis such as XRF or pXRF, and "source" artifacts, samples of, or whole assemblages in order to determine lithic procurement patterns. XRF or pXRF methods of analysis are preferred to other forms of geochemical analysis because they are relatively inexpensive once the equipment is purchased, and they are both non-destructive, a quality conducive to the proper preservation of the archaeological record. XRF and pXRF are especially useful when calibration and quantification standards are applied to the data set. Examples of XRF and pXRF studies utilizing calibration and quantification standards can be found around the world, but are especially common in South America.

Example of Successful XRF Studies: Obsidian in South America

Obsidian is an igneous rock formed from the rapid cooling of magma, resulting in an almost glass like stone (Weldon 2010). Because of its rapid formation process, obsidian is a highly homogenous material (Weldon 2010). This homogeneity in material type is preferred for sourcing studies using XRF or pXRF techniques (Drake 2014) Because of the nature of formation of sedimentary rocks such as silicified sandstone, or other lithic material such as cherts, these materials tend to be less homogenous. This lack of homogeneity is due to multiple

causes such as differing parent material for sedimentary rocks, differentiation in silica bodies which decayed to form silica dioxide in the stone, or the presence of mineral inclusion in the sample. Because obsidian lacks these issues, and exemplifies excellent homogeneity, obsidian has been used as the "pioneering" rock in refining geochemical analysis techniques and methodology (Andrefsky 2005:43-45; Drake 2014; Weldon 2010).

An obsidian sourcing study by Smith et al. (2007) conducted at several Middle and Late Post-classic sites in the Yautepec Valley of Mexico was able to successfully use XRF geochemical analysis (a non-destructive technique) and INAA (a destructive technique) to discern local and regional exchange networks, and how these networks and exchange systems changed over time for high quality obsidian. Although obsidian is homogenous in composition and silicified sandstones can be said to be heterogeneous in composition, his study successfully demonstrates that once methodology is refined and uniform, nondestructive forms of geochemical analysis (such as pXRF or XRF) offers the archaeologist a method to gather quantitative data. This data, when applied correctly can be used to discern human behavioral and social patterns in the past through the sourcing of lithic artifacts. The aim of this study is to determine if pXRF techniques of analysis used in obsidian sourcing studies like that of Smith et al. (2007) could be conducted on heterogeneous materials like silicified sandstones.

METHODS

Why Geochemically Source with pXRF?

Portable XRF sourcing is preferable to macroscopic analysis and destructive types of geochemical techniques because: 1) if the data is gathered and recorded properly the conclusions

made about sourcing will be accurate and backed by quantifiable scientific data and 2) this type of analysis is conductive to the preservation of the archaeological record in that it is non-destructive. Many macroscopic means of lithic sourcing rely on color, grain size, presence or lack of inclusions, translucency, luster, color pattern, and even magnetic response. These traits are the recorded and statistical analysis can then be performed to discern co-occurring traits, and create groups of probable sources within the sample being analyzed (Wendt 2015:1-2). However, certain lithic materials, such as silicified sandstones present a problem to many macroscopic sourcing techniques because silicified sandstones can exhibit a high degree of variation in color (see Figure 2), texture, translucency, and other facts, within sources. This varaition within sources, coupled with the lack of varaition between some sources may make identification of silicifed sandstones based on visual charcteristics problemeatic.

Figure 2: Sample of Hixton silicified sandstone from Silver Mound (display at the Mississippi Valley Archaeology Center) (Photo by Author).

For instance, during the sampling process at the Arcadia Ridge exposure a high degree of variation in color and grain size was observed. At this exposure, which was roughly 100 meters in length, the northern-most extent and down to last 20 meters was a dark golden brown. However, the last 20 meters were a much lighter almost semi-translucent gray (Figures 3,4,5).

Figure 3: Sample 1 from sample area 1, at northern-most end of outcrop at Arcadia Ridge (Photo by Author).

Figure 4: Samples from sample area 2, approx. 50m SE down outcrop from sample area 1 (Photo by Author).

Figure 5: Sample 7 from sample area 3, southern-most end of exposure of Arcadia Ridge outcrop. (note lighter color in this sample in contrast to darker samples from sample areas 1 & 2) (Photo by Author).

In addition, the Arcadia Ridge Hwy. 93 outcrop had a high degree of sorting of sand grains by size from largest to smaller going down the strata. This differentiation in grain size throughout the strata may lead to artifacts being derived from the same source with very different observable differences in grainsize. This example from my field experience illustrates that sources can contain a high degree of variability within the source, which may be misleading to lithic analysis using macroscopic techniques such as color, translucency, and grainsize to differentiate between source types. Conversely, it is also possible that certain silicified sandstone sources, such as Hixton and Cataract have low variation in observable traits because they both belong to the Wonewoc formation (Boszhardt 1993:3), making differentiation between the two very difficult at times. Because of the unreliability in objectively recording observable traits and the high variation in and between silicified sandstone sources, I believe that to most accurately source lithic assemblages, a form of geochemical analysis should be employed, especially if the

materials exhibit high degrees of variability within sources, and low degrees of variability between sources. Arcadia Ridge, Cataract, Hixton, and other silicified sandstones exhibit this kind of variability, making them prime candidates for geochemical sourcing studies.

Sampling: Discussion and General Procedures

In order to gather pXRF and ICP-MS data on UMRV silicified sandstones, three source locations of silicified sandstones (Arcadia Ridge, Cataract, and Hixton) were selected for sampling. Arcadia Ridge, Cataract, and Hixton silicified sandstones were selected for based on several factors including the relevance to the archaeological record, presence in literature (Boszhardt 1998; Boszhardt and Carr 2010), and the accessibility of these lithic materials to the author for sampling. In order to determine which sources would be best, I collaborated with several local collectors, as well as professional archaeologist, to determine which sources would be best for this project. Collaborations will be discussed in full detail in each description of sampling procedures at each locality. A specialized strategy was developed at each location to cater to the needs and problems presented by each location, as well as to gather the best samples possible with minimal destruction to the archaeological record.

During the course of collecting samples of Arcadia Ridge, Cataract, and Hixton for non-destructive and destructive analysis, several procedures remained constant. First, samples were selected with no cortex, or cortex that could be trimmed by flintknapping. This was done in order to prevent the elemental analysis of cortex. Cortex is the exterior chemically or mechanically weathered of tool stone surface not normally utilized for stone tool production. Cortex, in the past, was normally trimmed at quarry sites because it represented unusable material and therefore

is unlikely to make it back to non-quarry sites (Andrefsky 2005:103-106). My analysis, conducted on silicified sandstones using pXRF, prior to this study, demonstrated that the cortex of silicified sandstones differs significantly from the rest of the stone in elemental composition, therefore was important to exclude from my analysis in order to produce the most representative results. Second, it was important to ensure that the samples gathered were of the source origin being sought, especially at Silver Mound (the source of Hixton) and Cataract. At both of these locations materials were recovered from sampling were from "secondary context," not from "live" bedrock, and thus had the potential to be transported from another source location to the source location at which the sample was found. To ensure that samples recovered from sources were most likely of that source origin, the presence of cortex and "primary reduction flakes" were used as indicators of close to source knapping (Andrefsky 2005:103,187). Thus, samples that contained cortex, or could be described as "primary reduction flakes" were targeted during the sampling process. In addition, samples were also visually confirmed (to the best of my ability) to be of source origin based on a variety of physical properties such as color, grain size and shape, and translucency. Information on these attributes was gathered from the reference collection of lithic materials at the Mississippi Valley Archaeology Center (MVAC). Another aim during the sampling process was to collect as much variation in color found at each sampling area. The reasoning behind this was that elemental content influences color, and therefore a high range of color would mean a high range of elemental variation at each source, thus better characterizing each sources "elemental signature". All samples following collection in the field were hand-washed using a brush and water to ensure that soil and other debris which could influence elemental data were not present. In addition to the above mentioned sampling methods

each local source had particular sampling strategies, which were developed to provide a better elemental characterization of each source.

Arcadia Ridge

My sample area for Arcadia Ridge silicified sandstone comes from a modern exposure of lithic material along State Highway 93 (Figures 6, 7, 8 and 9).

Figure 6: Looking south down Arcadia Ridge Hwy 93 outcrop (Google Earth 2016).

Figure 7: Sample area 2 at Arcadia Ridge Hwy. 93 outcrop (Photo by Author).

Figure 8: Exposed Arcadia Ridge silicified sandstone (Photo by Author).

Figure 9: Distal (southern-most) end of Arcadia Ridge Hwy. 93 exposure (Photo by Author).

The location of this exposure was provided by avocational archaeologist Dan Wendt. This exposure runs approximately 100m long. Samples were derived directly from the "live bed-rock." The location of each sample area was photographed before and after and the location of

each sample was recorded using hand-held GPS. Sample were each bagged individually according to provenience information. Samples collected that were too large to fit within pXRF screening area were knapped to size by the author using antler.

Cataract

Local collector Todd Reichart and myself completed a series of pedestrian surveys around the Cataract locality with to collect samples of silicified sandstone to conduct pXRF and inductively coupled plasma spectroscopy (ICP-MS) analysis. Cataract was targeted as a locality due to its probable prehistoric importance, inferred from the extensive extraction of this material at Walzack-Wontor (Boszhardt 1998). Because of this probable prehistoric importance and accessibility, 12 samples of silicified sandstone were recovered from surface surveys conducted around the Cataract locality on properties which we had received the landowner's permission to sample (see Figure 10). These 12 samples were deemed likely to have originated from, local outcrops of Cataract silicified sandstone based on physical properties, proximity to sources, and the presence of cortex, an indicator of primary reduction in the lithic sequence (Andrefsky 2005). All samples appear to be archaeological in nature. When selecting specimens, flat specimens were selected over less flat ones (pXRF readings are more consistent from flatter samples) and a range of colors were selected in an attempt to cover the color (and in turn elemental) variation encompassed by Cataract silicified sandstone. Tools and culturally diagnostic materials were selected against, and "important" or protected areas (such as Walzack-Wontor) were avoided. Samples were photographed in-situ (see Figure 11) and provenience data in the form of GPS co-ordinates were gathered for every sample, excluding sample 9 (GPS co-ordinates were not collected due to proximity to sample 8). Samples were also photographed after cleaning in a lab setting (see Figure 12).

Figure 10: View of sample area 1 at Cataract locality (Photo by Author).

Figure 11: Sample 4 from Cataract locality (pink on ruler points north) (Photo by Author).

Figure 12: Sample 1 from Cataract locality (note cortex, which was trimmed prior to ICP-MS analysis) (Photo by Author).

Hixton

After gaining permission from Paul Gardner of The Archaeological Conservancy, I collected 11 small samples of Hixton silicified sandstone (or othroquartzite) from the surface of Silver Mound. Silver Mound, the source of Hixton silicified sandstone, is a heavily utilized archaeological complex throughout all of prehistory (Boszhardt and Carr 2010; Lang 1987). This become apparent quickly as artifacts are fairly abundant on the surface and features made from the extraction of materials can be found with ease (Figure 13).

Figure 13: Quarry pit at Silver Mound, the source of Hixton silicified sandstone (Photo by Author).

All samples appear to be archaeological in nature. When selecting specimens a range of colors was selected in an attempt to cover the color (and in turn elemental) variation encompassed by Hixton silicified sandstones. No tools or culturally diagnostic items were selected for sampling. Also, "important" areas such as rockshelters, quarry pits, or any other visible features were avoided during the sampling process. Each sample was photographed in situ before removal, and the location of each sample was recorded using hand-held GPS. Samples were each bagged individually according to provenience information. Samples collected that were too large to fit within pXRF screening area or that contained cortex were knapped to size by the author using antler, with their provenience information being retained and as much as "waste" possible being kept. Figures 14, 15, and 16 show various Hixton samples both in field and lab setting.

Figure 14: Sample 3 in situ at Silver Mound (Photo by Author).

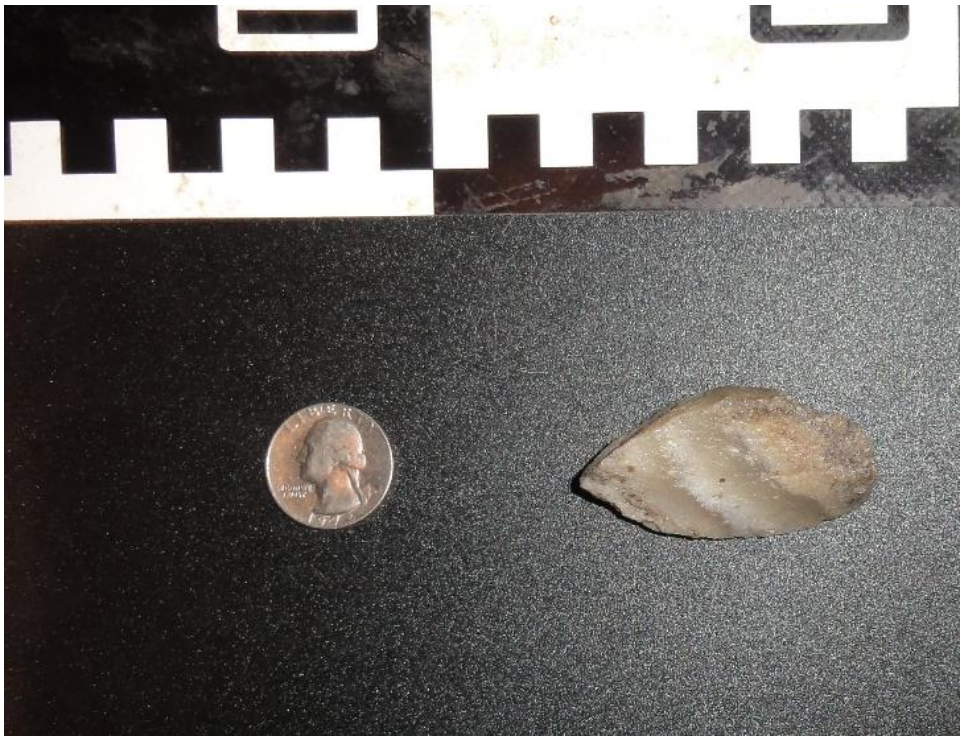

Figure 15: Sample 3 from Silver Mound in lab setting (Photo by Author)

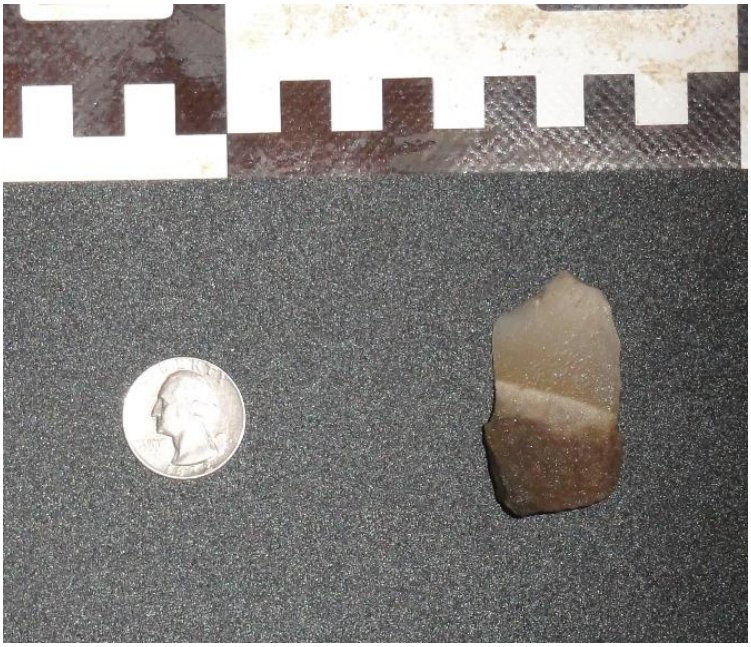

Figure 16: Sample 8 from Silver Mound. Cortex was trimmed prior to ICP-MS analysis (Photo by Author).

Why use Portable X-Ray Fluorescence (pXRF)?

Portable XRF is a preferred technology for geochemical sourcing studies in that it can provide accurate, real-time results, and is completely non-destructive. Portable x-ray fluorescence has the advantage to lab-based XRF in that pXRF is portable and can be utilized at sites and on surveys, as opposed to stationary XRF, which requires artifacts be transported to the machine. Portable XRF, in general, operates by filling the sample being analyzed with X-rays. This energy charge "excites" electrons of elements in the samples, causing them to jump energy levels. Electrons jumping to higher energy levels releases fluorescent energy, or what Andrefsky calls "secondary X-rays" (Andrefsky 2005:44). Each element has its own energy characterization or "intensity of secondary x-rays" (Andrefsky 2005:44). This information is then recorded by the pXRF and can provide the user with information concerning the concentration of elements in the sample (Andrefsky 2005:44). One problem with pXRF is that without a calibration system,

pXRF does not provide qualitative data, or information concerning elemental composition in ppm. Instead raw pXRF data only provides inferred elemental values captured from "secondary x-rays" (Andrefsky 2005:44). This raw data is displayed in the form of a spectra like that shown in Figure 17, with peaks along the x-axis corresponding to individual elements and their height on the y-axis representing their relative values.

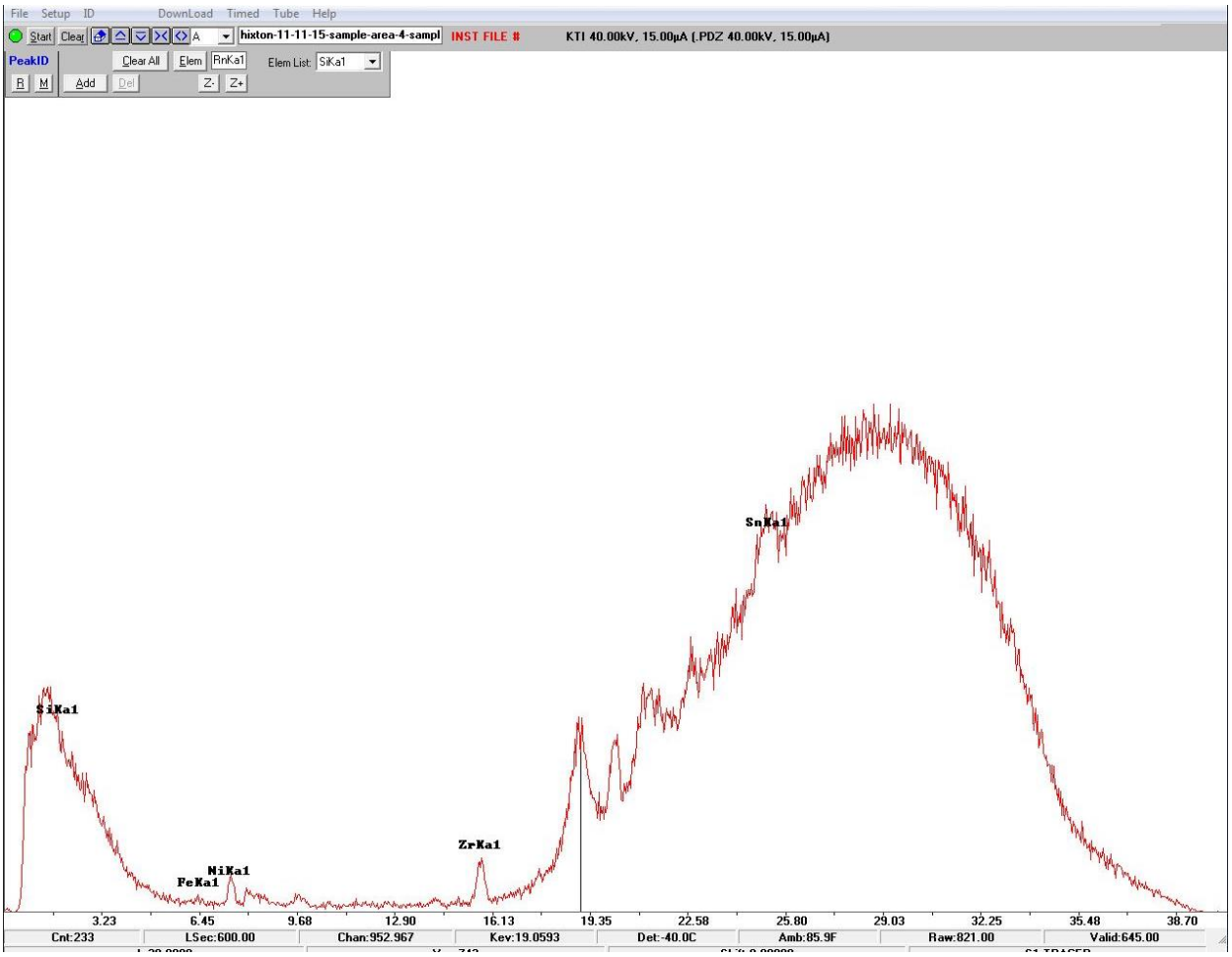

Figure 17: Raw pXRF spectra, elements are plotted on x-axis and their relative values on the y-axis.

The raw, unquantified spectra produced by the pXRF provides the analyst with little useful information that could aid in the elemental characterization and thus differentiation between lithic sources. However, spectra can be calibrated and quantified by developing a calibration and

quantification with a sample of data in ppm. I chose to use ICP-MS data to calibrate raw pXRF results in a spreadsheet ran with S1 pXRF calibration software to produce calibration and quantification standards. These standards were applied to raw spectra to obtain quantified data, in ppm, which could then be used to elementally characterize and differentiate between Arcadia Ridge, Cataract, and Hixton silicified sandstones.

Why use Inductively Coupled Plasma Mass Spectroscopy (ICP-MS)?

Inductively Coupled Plasma Mass Spectroscopy is a geochemical technique often employed in lithic sourcing studies. ICP-MS, in general, works by heating the sample in a solution to 6000°C. This cause the elements within the sample to burn at a specific and unique color. These colors are then separated and their intensity is analyzed by the mass spectrometer, providing ppm data on the elemental composition of that sample (Price and Burton 2011:84). ICP-MS, unlike pXRF, is a destructive technique of analysis, in that the sample is ground and dissolved into a solution which is then heated to an extremely high temperature (Price and Burton 2011:84). Because of this I argue that pXRF is a preferred method of geochemical sourcing in comparison to ICP-MS. However, ICP-MS data can be particularly useful in developing a calibration curve for pXRF results, which in turn can be used to provide qualitative data on sample composition from pXRF analysis alone. This study used a sample of ICP-MS data obtained from ALS Chemistry labs to calibrate and quantify the pXRF results in a spreadsheet run through S1 pXRF calibration software.

pXRF Analysis

The pXRF instrument used for this study is a Bruker Tracer model III-V housed in the Geography department at the University of Wisconsin-La Crosse. After gathering, recording, and

preparing samples each sample was subjected to three pXRF scans. Each sample was scanned each time in a different location to ensure that the collective scans were capturing as much of the sample as possible in the spectra. Special attention was paid to avoiding cortex and inclusions that would not be included in ICP-MS analysis. These areas were excluded in analysis in that they represent areas of the rock not utilized for stone tool production. Each scan was 10 minutes in length at energy settings 40 kV, a current of 15 μA, and a pulse length of 199. A green filter composed of 12mil Al, 1 mil Ti, 6 mil Cu was utilized during each scan. Through personal communication with Joshua Keene of Texas A&M I learned that the green filter is useful in lithic sourcing studies involving trace element analysis because it works to mask lighter elements such as silicon that aren't useful in differentiating between sources, and also works to excite heavier elements, making them more susceptible to recordation by the pXRF (Keene, personal communication: 2015). Each scan was saved as a .pdz file (specific file type for "raw" pXRF spectra) and grouped together by source to await entry into the S1pXRF calibration software.

ICP-MS Analysis

To obtain known values for a sample of silicified sandstones 16 samples were sent to ALS Chemistry Labs for ICP-MS analysis following analysis via pXRF. In order to gather data on all elements of interest a range of ICP-MS methods were used. The following service codes correspond to the analysis type performed by ALS, ME-MS81, ME-ICP06, and ME-ICP61**.** The description of these methods, in detail, can be found on ALS Chemistry Labs website (alsglobal.com). Appendix 1 shows all ICP-MS samples and their corresponding data in its entirety. Appendix 2 is a concise version of Appendix 1; displaying all samples used, and the corresponding values (in ppms) of elements deemed useful to this study. All ICP-MS values that

fell below the level of detection (any values with a "<") was changed to the value of "0" for graphing and statistical purposes.

Table 3 – displaying samples withheld for calibration and validation. SM = Silver Mound (Hixton), Cat. = Cataract, AR = Arcadia Ridge.

Calibration	Validation
-AR-SA1-S-1-F-2	**-AR-SA2-S-4**
-AR-SA2-S-2	**-AR-SA2-S-5**
-AR-SA3-S-7	**-Cat.-S-8**
-Cat.-S-1	**-SM-SA3-S-7**
-Cat.-S-2	**-SM-SA4-S-8**
-Cat.-S-5	**-SM-SA5-S-11**
-Cat.-S-7	
-SM-SA1-S-2	
-SM-SA2-S-5	
-SM-SA5-10	

Calibration

To create a calibration for unquantified pXRF scans the elemental values (in ppm) for 16 samples of silicified sandstones obtained from ICP-MS analysis were inserted into the S1pXRF calibration program. As shown in Table 3, ten samples and their values were used to establish calibration standards while six samples were withheld to use for the validation of this calibration. After using the S1pXRF calibration program and an excel spreadsheet with formatting provided

by Dr. Colin Belby of the University of Wisconsin-La Crosse's Geography and Earth Sciences Department to create and validate the calibration, the calibration was then applied to uncalibrated pXRF scans. Calibrated values (in ppm) were then obtained for each pXRF scan of every sample gathered. This totals 24 calibrated scans for Arcadia Ridge, 33 calibrated scans for Cataract, and 33 calibrated scans for Hixton silicified sandstone, making the total sample size 90 scans. Calibrated values for these scans are provided in Appendix 4, this table includes only elements that were identified as being potential useful to differentiating between silicified sandstones.

RESULTS

First, this study was able to demonstrate that calibrated and quantified pXRF results can be a good analog to ICP-MS results in the case of the four elements (Chromium, Nickel, Lead, and Zinc) although to varying degrees. These four elements were used to differentiate Arcadia Ridge, Cataract, and Hixton silicified sandstone in this study. To validate calibration standards one must demonstrate that there is little variation between ICP-MS results and calibrated and quantified pXRF results. In this case a R^2 value of 1 represents a perfect correlation between pXRF and ICP-MS detection, so values closer to 1 represent less variation between detection abilities in pXRF and ICP-MS analysis, and therefore more accurate calibration and quantification standards. In order to determine the validity of my standards I plotted all 16 ICP-MS values for each element against a random sample of a corresponding calibrated pXRF scans and then determined the R^2 value for each of my elements deemed useful for to this study (Ba, Co, Cr, La, Ni, Pb(La1), Pb(Lb1), Sr, Zn, and Zr).

Figure 18 shows the variation for nickel (Ni) level detection between ICP-MS results and calibrated pXRF scans (taken from the NiKa1 energy level).

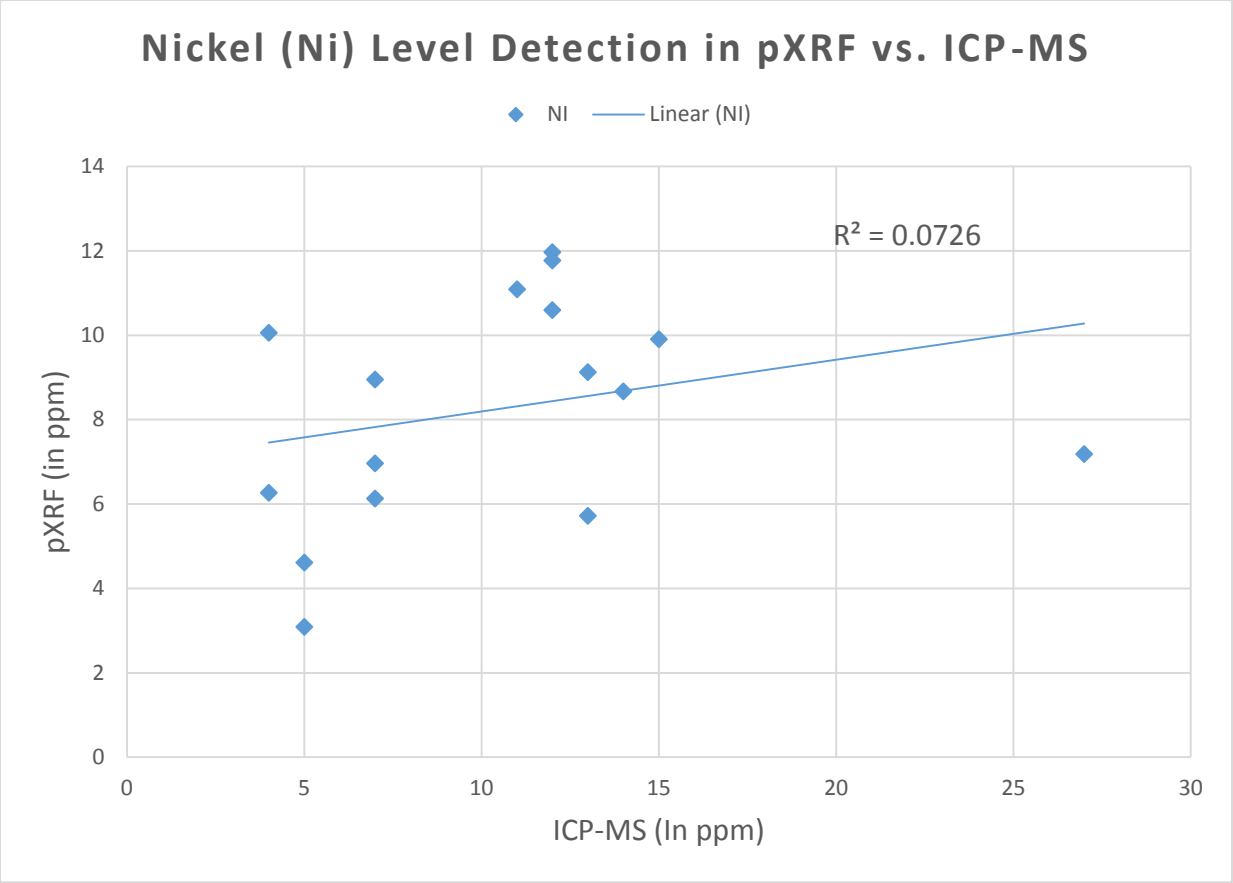

Figure 18: Scatter plot showing regression between pXRF and ICP-MS detection of nickel. Each point corresponds to a ICP-MS result and its corresponding calibrated pXRF scan.

The R^2 value from the linear regression on this scatter-plot shows that nickel has a low R^2 value ($R^2 = 0.0726$). Meaning that nickel level detection via pXRF analysis produces different results then nickel analysis through ICP-MS, making nickel detection from pXRF analysis less reliable than nickel detection from ICP-MS analysis.

Figure 19 shows the variation between lead (Pb) level detection between ICP-MS results and calibrated pXRF scans (taken from the PbLa1 energy level).

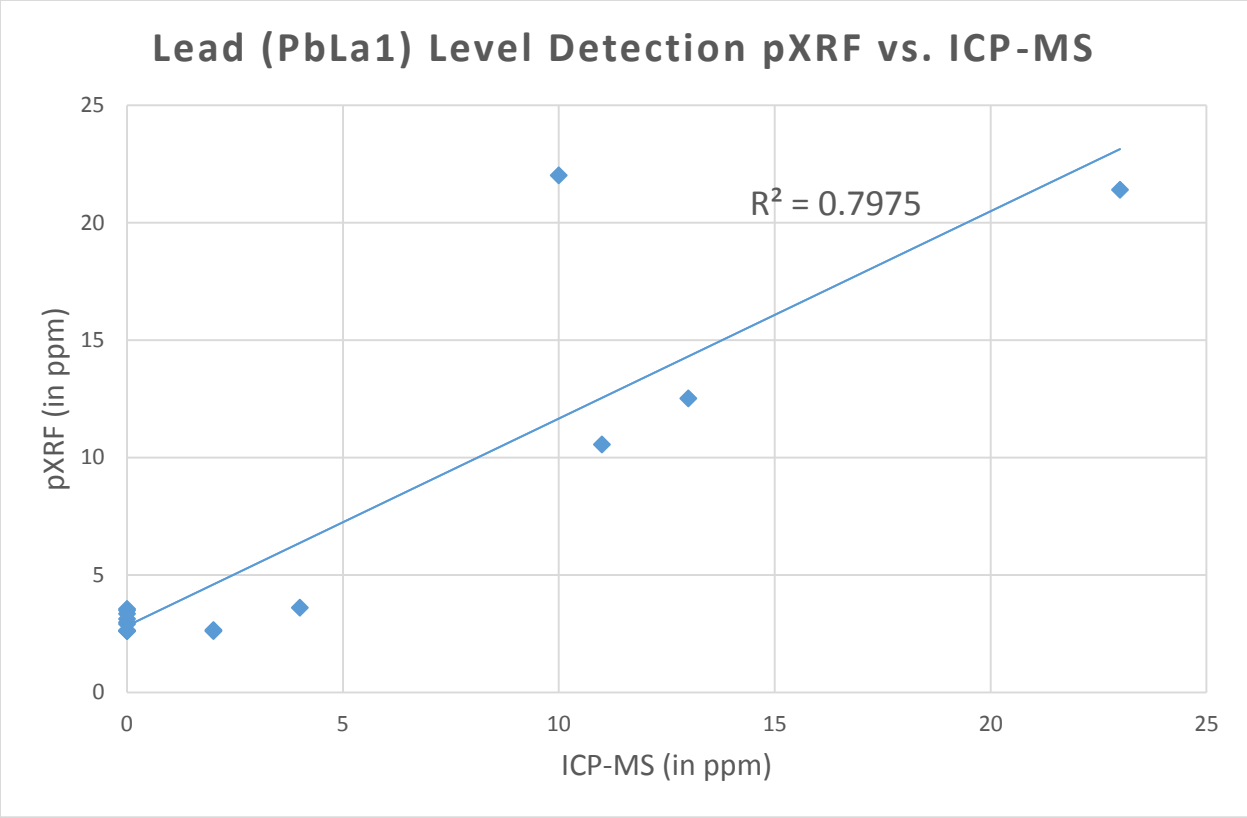

Figure 19: Scatter plot showing regression between pXRF and ICP-MS detection of lead. Each point corresponds to a ICP-MS result and its corresponding calibrated pXRF scan.

The R^2 value from the linear regression on this scatter-plot shows that the comparison of lead level detection, from the PbLa1 energy level, results in a relatively high R^2 value ($R^2 = 0.7975$). This means that lead detection from calibrated pXRF analysis, using the PbLa1 energy level, is a good analog for lead detection via ICP-MS analysis, because these methods produce similar results.

Figure 20 shows the variation between lead (Pb) level detection between ICP-MS results and calibrated pXRF scans (taken from the PbLb1 energy level).

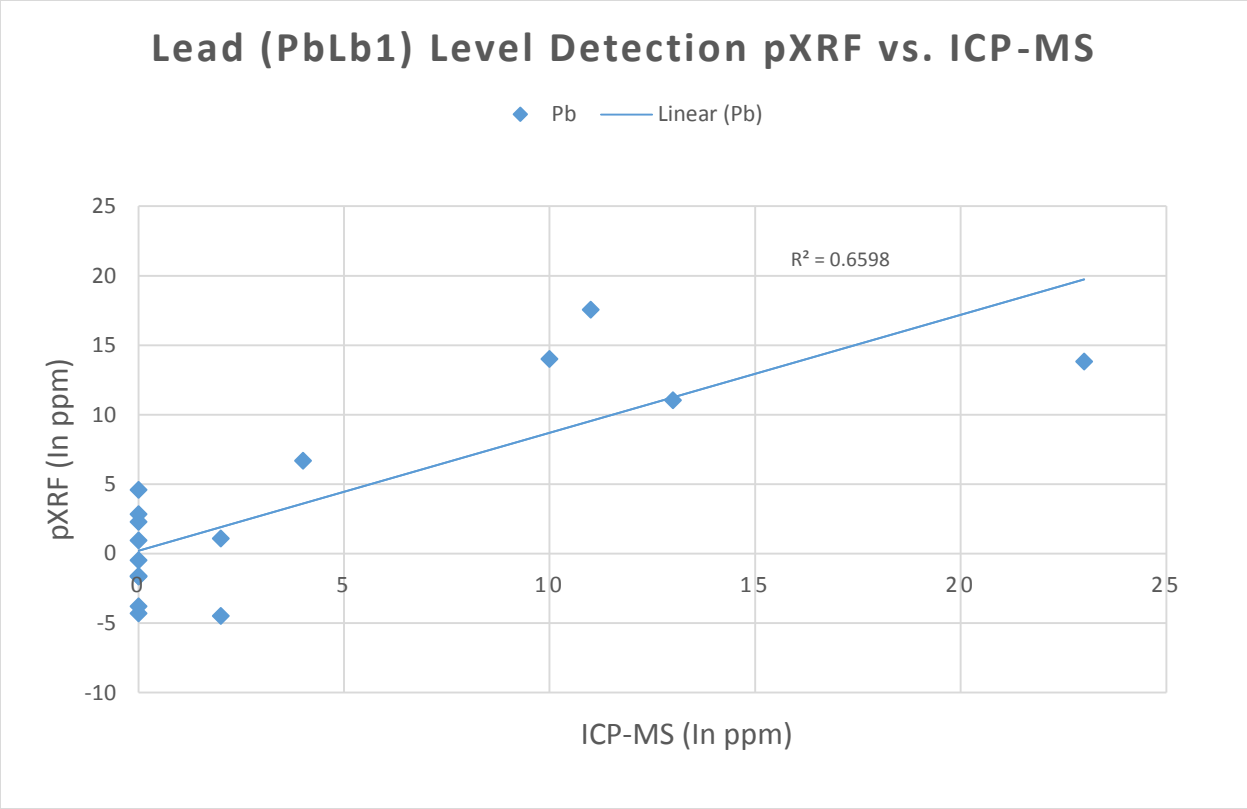

Figure 20: Scatter plot showing regression between pXRF and ICP-MS detection of lead. Each point corresponds to a ICP-MS result and its corresponding calibrated pXRF scan.

The R^2 value from the linear regression on this scatter-plot shows that the comparison of lead level detection, from the PbLb1 energy level, results in a fairly high R^2 value ($R^2 = 0.6598$). This means that lead detection from calibrated pXRF results, using the PbLb1 energy level, is a good analog for lead detection via ICP-MS analysis, because these methods produce similar results. However, PbLa1 detection, from calibrated pXRF results, produce results most similar to ICP-MS (Figure 24), making PbLa1 the preferred energy level for measuring lead content through pXRF analysis.

Figure 21 shows the variation between strontium (Sr) level detection between ICP-MS results and calibrated pXRF scans (taken from the SrKa1 energy level).

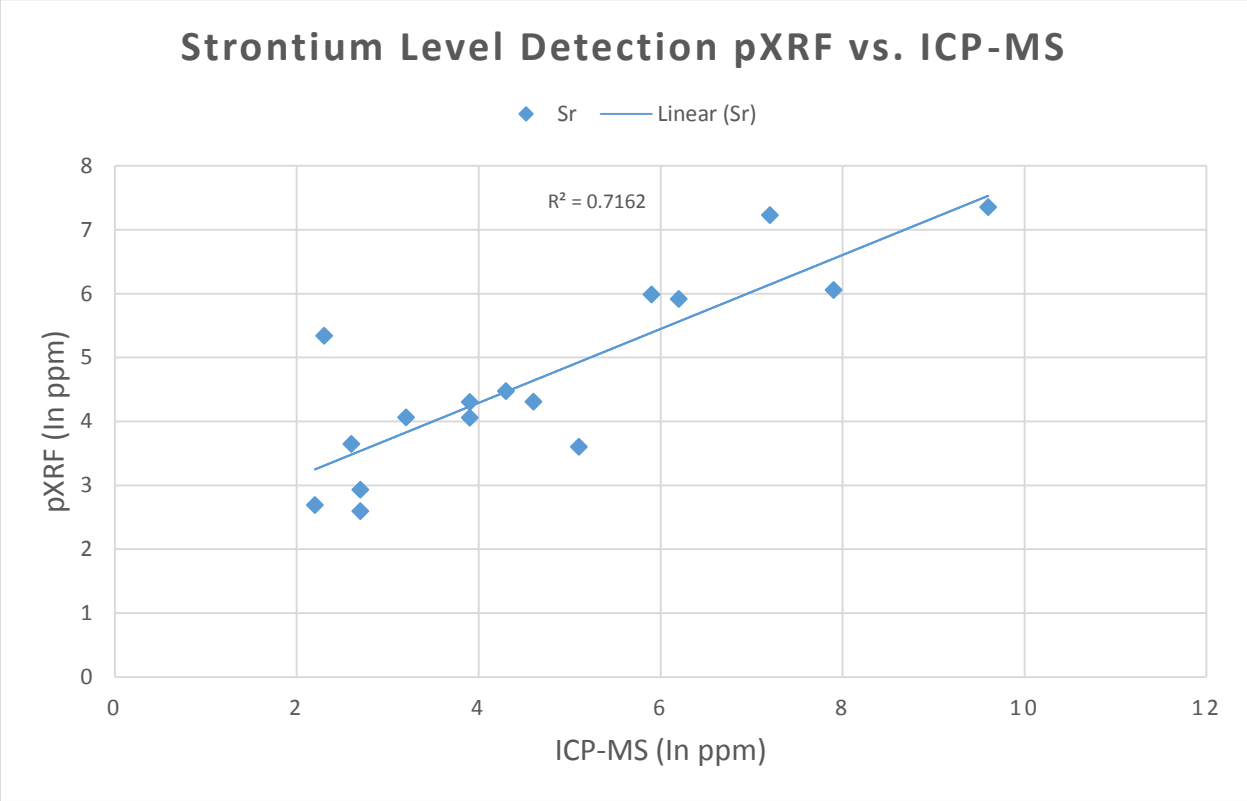

Figure 21: Scatter plot showing regression between pXRF and ICP-MS detection of strontium. Each point corresponds to a ICP-MS result and its corresponding calibrated pXRF scan.

The R^2 value from the linear regression on this scatter-plot shows that strontium has a relatively high R^2 value ($R^2 = 0.7162$). Meaning that strontium level detection via pXRF analysis produces similar results to strontium analysis through ICP-MS. Meaning that strontium detection through pXRF analysis can be considered to produce reliable results.

Figure 22 shows the variation between zinc (Zn) level detection between ICP-MS results and calibrated pXRF scans (taken from the ZnKa1 energy level).

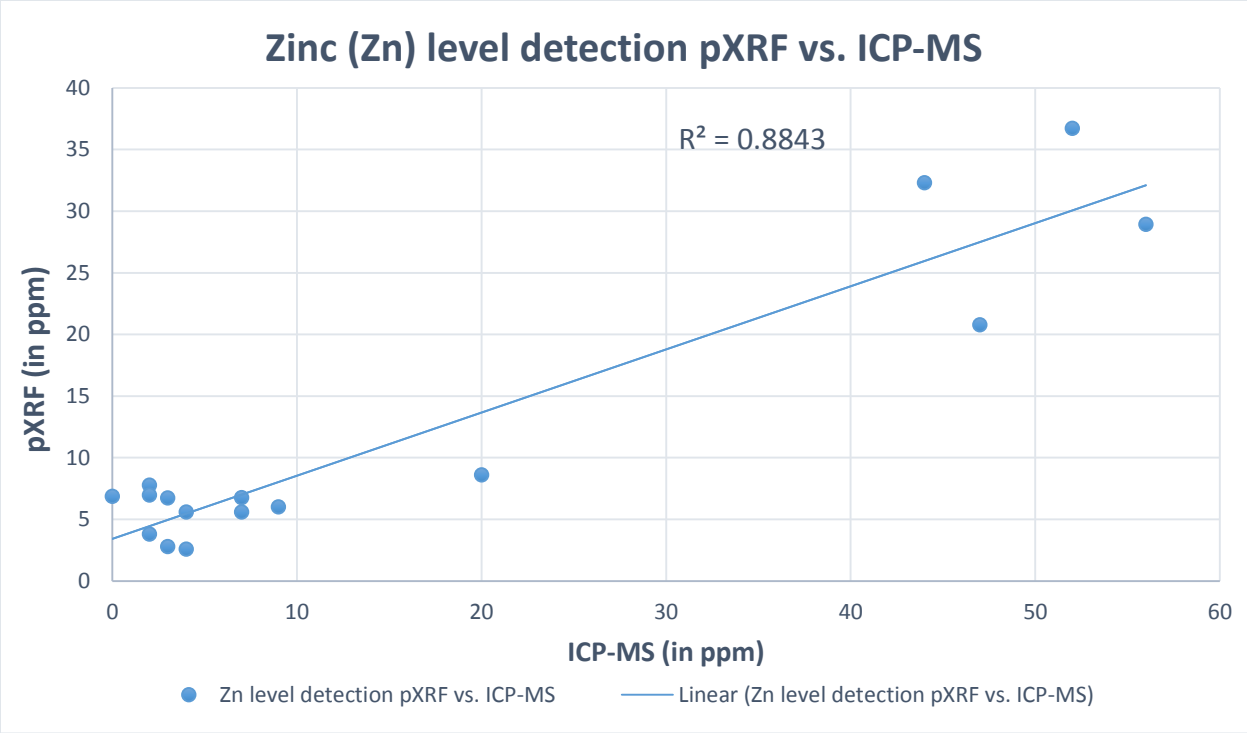

Figure 22: Scatter plot showing regression between pXRF and ICP-MS detection of zinc. Each point corresponds to a ICP-MS result and its corresponding calibrated pXRF scan.

Zinc detection between pXRF and ICP-MS analysis displays a relatively high R^2 value (R^2 = 0.8843). This means that zinc detection via calibrated pXRF displays little difference in results produced compared to ICP-MS results from the same samples, therefore, zinc detection through pXRF analysis can be considered to produce reliable results.

Figure 23 shows the variation between zirconium (Zr) level detection between ICP-MS results and calibrated pXRF scans (taken from the ZrKa1 energy level).

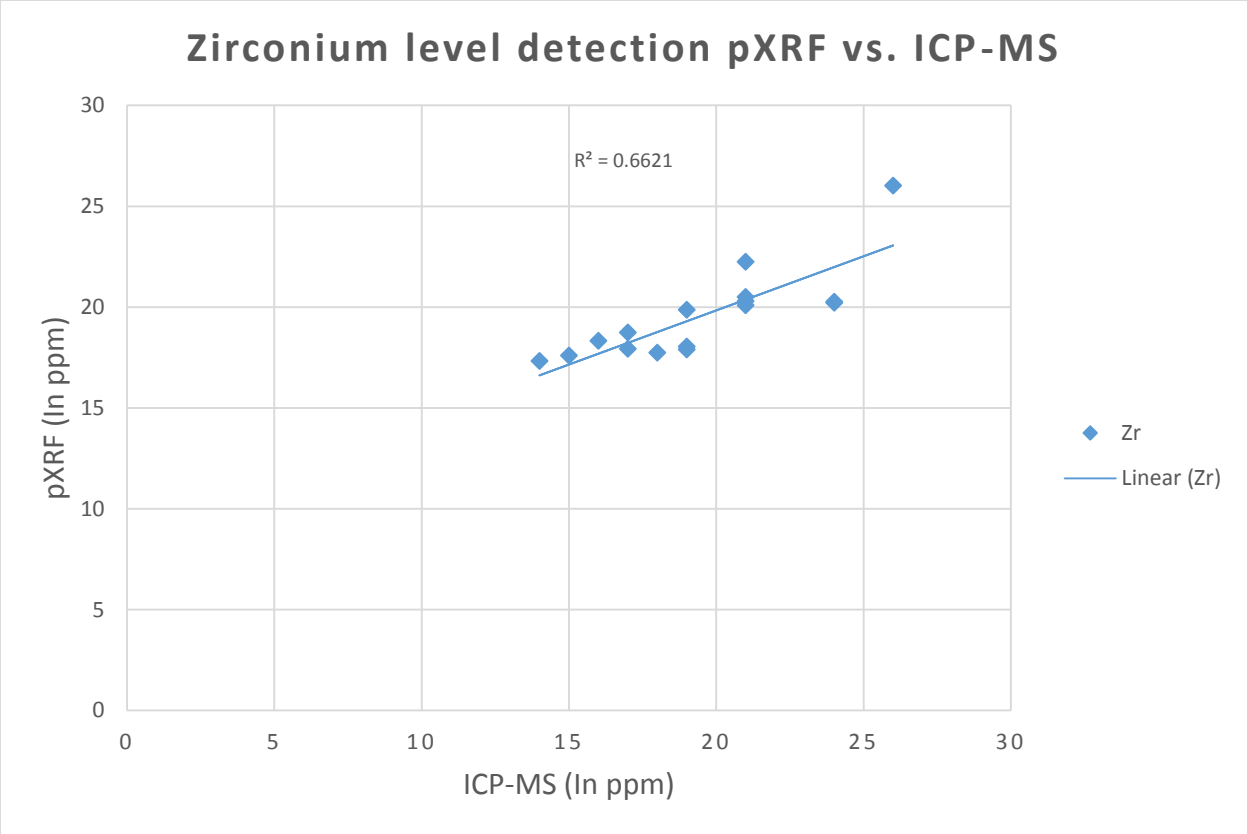

Figure 23: Scatter plot showing regression between pXRF and ICP-MS detection of zirconium. Each point corresponds to a ICP-MS result and its corresponding calibrated pXRF scan.

Zirconium detection between pXRF and ICP-MS analysis displays a relatively high R^2 value (R^2 = 0.6621). This means that zirconium detection via calibrated pXRF displays little difference in results produced compared to ICP-MS results from the same samples, therefore, zirconium detection through pXRF analysis can be considered to produce reliable results.

Figure 24 shows the variation between barium (Ba) level detection between ICP-MS results and calibrated pXRF scans (taken from the BaLa1 energy level).

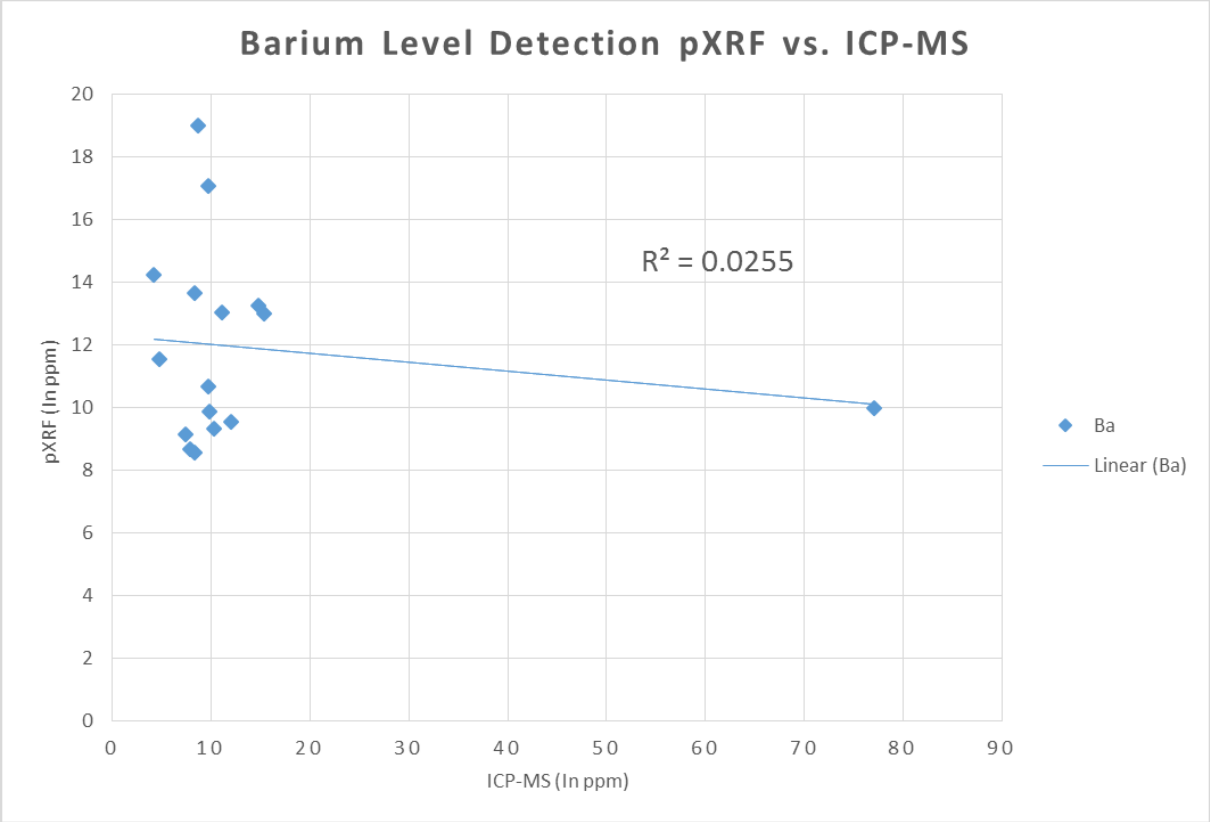

Figure 24: Scatter plot showing regression between pXRF and ICP-MS detection of barium. Each point corresponds to a ICP-MS result and its corresponding calibrated pXRF scan.

This linear regression of data from pXRF and ICP-MS for the element barium results in a relatively low R^2 value ($R^2 = 0.025$). This means that barium detection via calibrated pXRF is a not a good analog for barium detection via ICP-MS analysis, because these methods produce differing results.

Figure 25 shows the variation between cobalt (Co) level detection between ICP-MS results and calibrated pXRF scans (taken from the CoKa1 energy level).

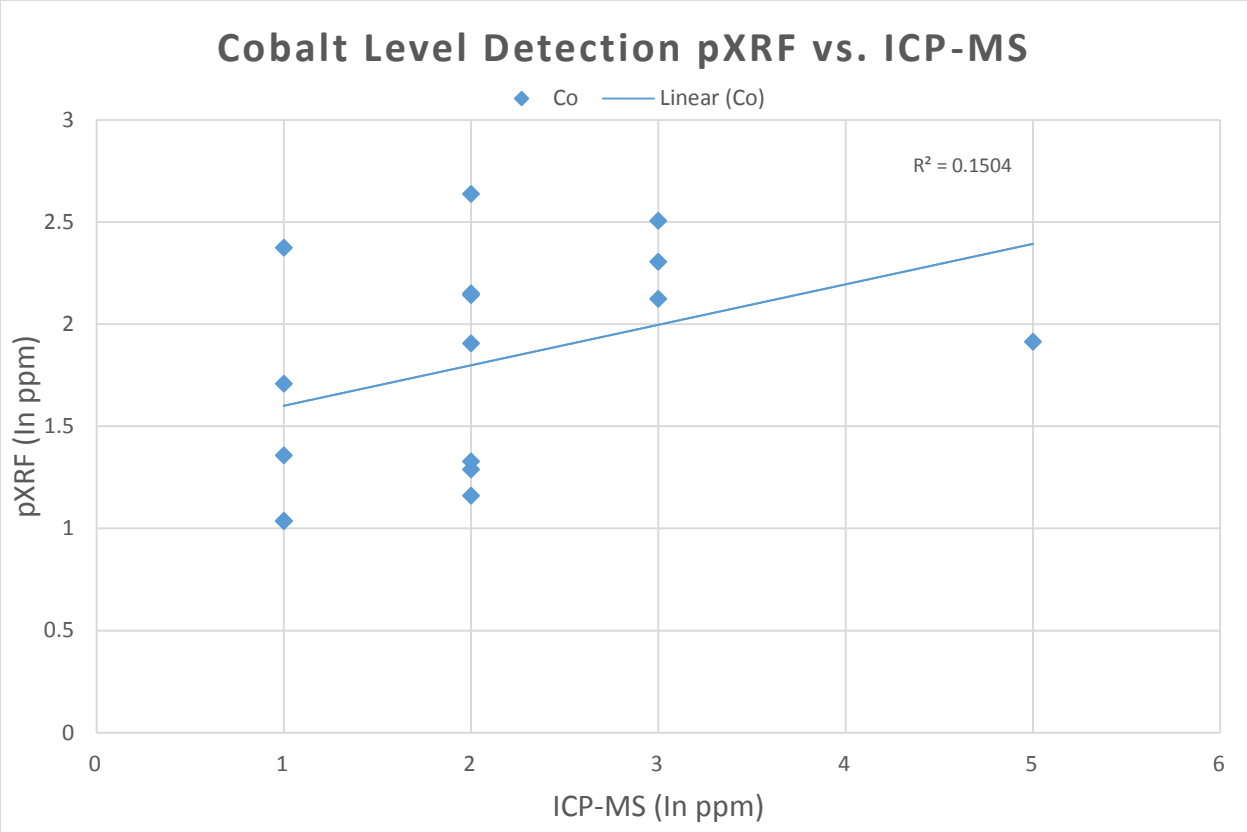

Figure 25: Scatter plot showing regression between pXRF and ICP-MS detection of cobalt. Each point corresponds to a ICP-MS result and its corresponding calibrated pXRF scan.

The linear regression of data from pXRF and ICP-MS for the element cobalt results in a relatively low R^2 value ($R^2 = 0.1504$). This means that cobalt detection, like barium detection via calibrated pXRF, is a not a good analog for cobalt detection via ICP-MS analysis because these methods produce different results.

Figure 26 shows the variation between chromium (Cr) level detection between ICP-MS results and calibrated pXRF scans (taken from the CrKa1 energy level).

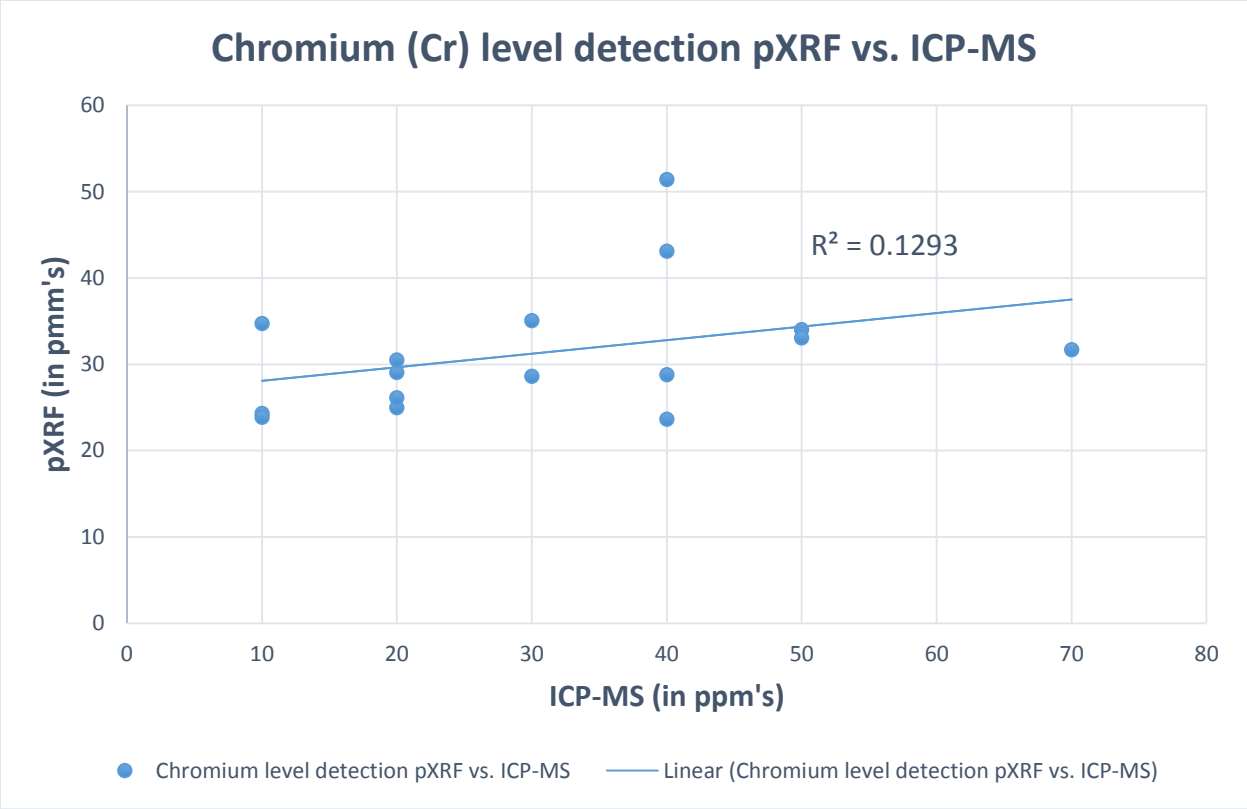

Figure 26: Scatter plot showing regression between pXRF and ICP-MS detection of chromium. Each point corresponds to a ICP-MS result and its corresponding calibrated pXRF scan.

This linear regression of data from pXRF and ICP-MS for the element chromium results in a low R^2 value ($R^2 = 0.1293$). These results demonstrate that pXRF and ICP-MS analysis produce different results for chromium detection. Therefor pXRF results for chromium are less reliable than ICP-MS results for chromium detection.

Figure 21 shows the variation for lanthanum (La) level detection between ICP-MS results and calibrated pXRF scans (taken from the LaLa1 energy level).

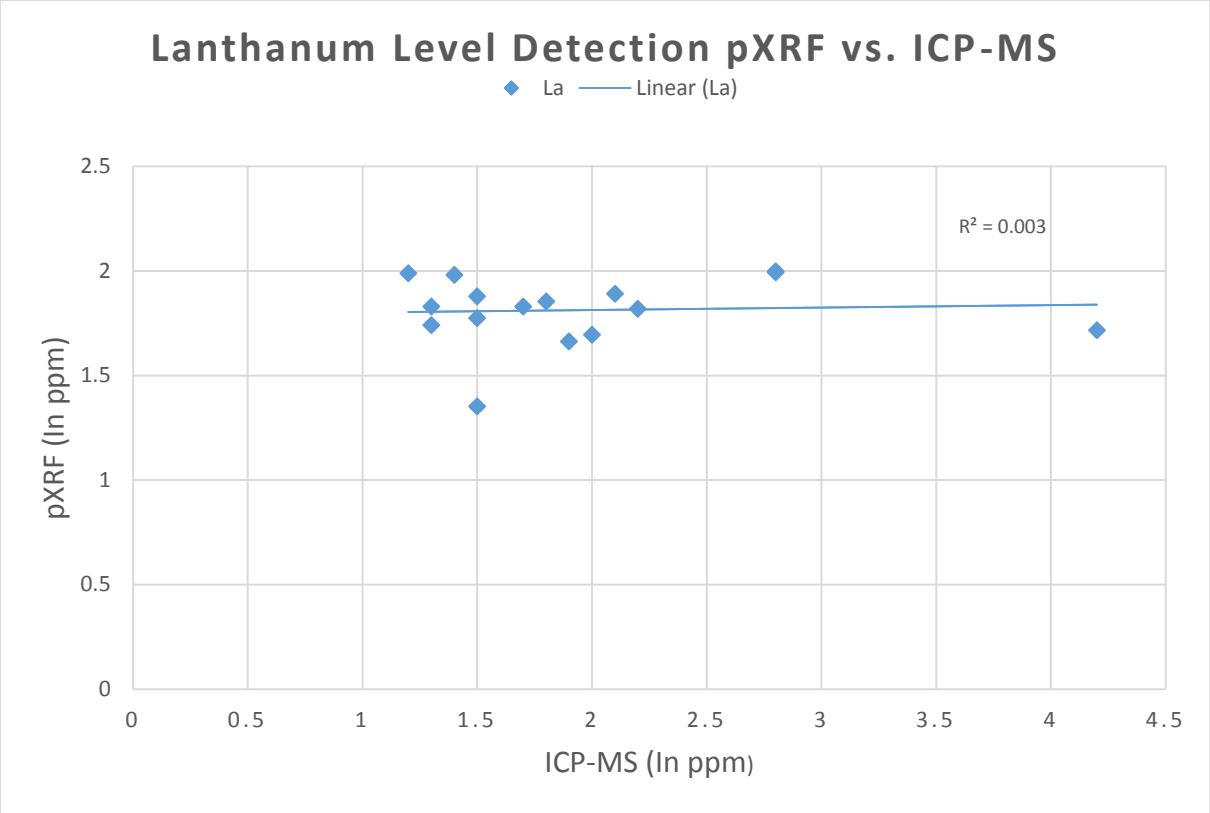

Figure 27: Scatter plot showing regression between pXRF and ICP-MS detection of lanthanum. Each point corresponds to a ICP-MS result and its corresponding calibrated pXRF scan.

This linear regression of data from pXRF and ICP-MS for the element lanthanum results in a low R^2 value ($R^2 = 0.003$). These results demonstrate that pXRF and ICP-MS analysis produce different results for lanthanum detection. Therefore, pXRF results for lanthanum detection are less reliable than ICP-MS results for lanthanum detection.

While lead (from both the PbLa1 and PbLb1 energy levels), strontium, zinc, and zirconium display little difference in detection between pXRF and ICP-MS analysis, barium, chromium, lanthanum, and nickel detection produce differing results between pXRF and ICP-MS analysis. Therefore, pXRF analysis is a reliable method for measuring lead, strontium, zinc, and zirconium concentrations in silicified sandstones, while pXRF is significantly less reliable for measuring barium, chromium, cobalt, lanthanum, and nickel in silicified sandstones.

Initial results demonstrate that, by using ICP-MS data, in conjunction with pXRF to create a calibration, reliable pXRF results can be obtained for some elements (Pb, Sr, Zn, and Zr), these results than can be used to describe elemental variation between sources at the formation level. These results illustrate that elements Pb (lead) and Zn (Zinc) may be useful in pXRF analysis in differentiating between Jordan formation (Arcadia Ridge) and Wonewoc formation (Hixton and Cataract) silicified sandstones. Tables 5, 6, and 7 provide the means, standard errors, standard deviations, maximum values, minimum values, and ranges (in ppms) by element derived from all calibrated pXRF scans for each source.

First, several differences emerge following the comparison of the mean values of lead (calculated from the PbLa1 energy level) between these three silicified sandstone sources. First, Arcadia Ridge silicified sandstone, a Jordan formation silicified sandstone displays a higher mean value for lead levels (21.26 ± 5.94 ppm) than both Cataract (2.92 ± 0.09 ppm) and Hixton (3.55 ± 0.21 ppm) silicified sandstones do, both of which belong to the Wonewoc formation. Because of this higher lead values, relative to Hixton and Cataract silicified sandstones, may be indicative of Arcadia Ridge silicified sandstone. Also zinc, (Zn) occurs in much higher levels in Arcadia Ridge silicified sandstone (mean= 35.35 ± 3.96 ppm), whereas Cataract (6.58 ± .43 ppm) and Hixton (6.36 ± .59 ppm) are much lower (Tables 5, 6, and 7). Zinc then is extremely useful in differentiating between Jordan and Wonewoc formation silicified sandstones. With high zinc levels being indicative of Jordan formation silicified sandstone such as Arcadia Ridge. Figure 28 illustrates that combining lead and zinc in analysis is useful in separating Arcadia Ridge silicified sandstones from Wonewoc formation silicified sandstones, but little separation between Cataract and Hixton silicified sandstones.

The outlier in Figure 28, Arcadia Ridge sample-1-flake-2-scan-3, represents a scan of cortex left on the sample. This sample shows higher than average zinc (Zn) and lead (Pb) values, causing it to fall out of the cluster of Arcadia Ridge samples. This illustrates that cortex is not a reliable surface to conduct pXRF analysis on, in that it represents a part of the stone that is elementally different.

Scatterplots were made for every element in the fashion of Figure 28 to try and discern clusters which would indicate variation useful for geochemical sourcing. The only elements analyzed from this study to yield any useful clustering are lead (Pb), strontium (Sr), and Zinc (Zn). Figure 29 is a termary plot showing the relative levels of Pbka1, SrKa1, and ZnKa1 from each scan in proportions. Proportions of each element were calculated by dividing each value by the sum of the three values from each scan and then multiplying that value by 100. The outlier shown in Figure 28 was excluded from the data set to make Figure 29. Figure 29 shows distinct clustering between Jordan formation (Arcadia Ridge) and Wonewoc formation (Cataract and Hixton) silicified sandstones. This clustering is cause by Arcadia Ridge silicified sandstone having lower strontium (SrKa1) levels, and higher lead (PbLa1) levels relative to Cataract and Hixton silicified sandstone.

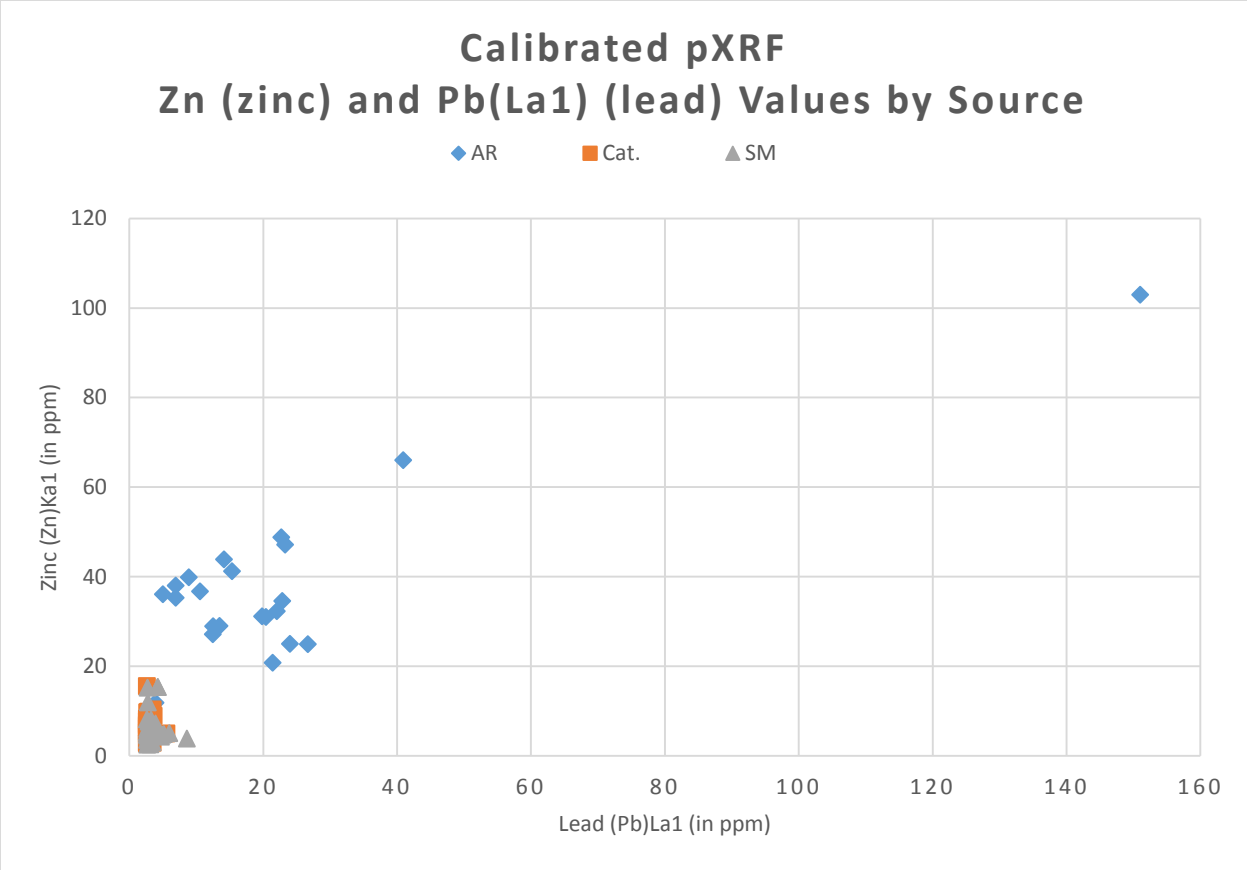

Figure 28: Each point corresponds to pXRF scan, note separation in Arcadia Ridge from Wonewoc formation silicified sandstones Hixton and Cataract.

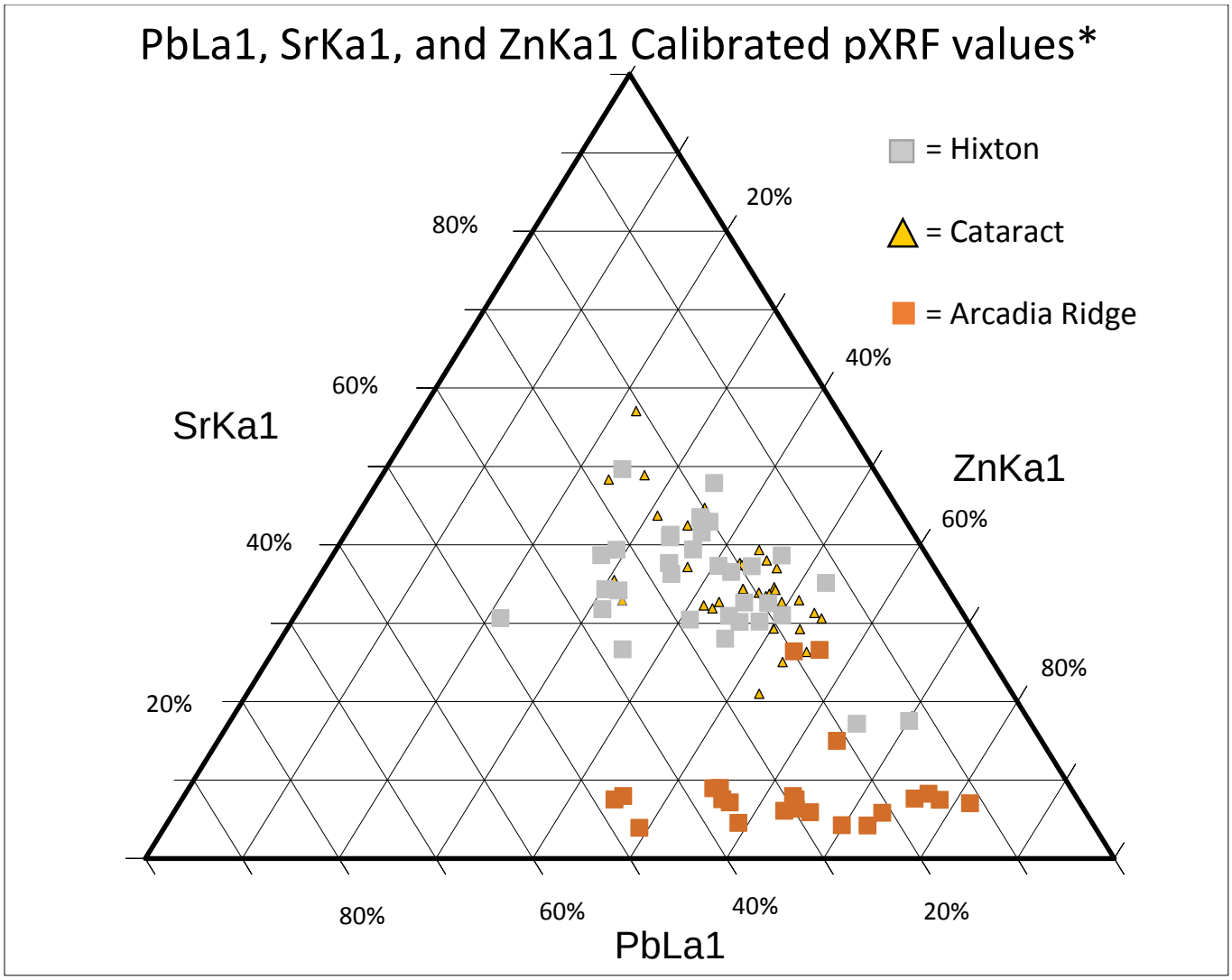

Figure 29: Temary plot showing proportions of PbLa1, SrKa1, and ZnKa1 from calibrated pXRF values. Every data point corresponds to an individual pXRF scan. Proportions of each element calculated by dividing each value by the sum of the three values from each scan and then multiplying that by 100.

Tables 5, 6, and 7: Statistical values (in ppms) for each element by silicified sandstone source. SE= Standard Error, SD= Standard Deviation

Table 5 **Arcadia Ridge**

	Mean	SE	SD	Maximum	Minimum	Range
Elements						
Ba	12.01	0.60	2.94	19.00	7.54	11.46
Co	3.68	1.11	10.13	50.92	1.04	49.88
Cr	27.11	2.07	5.44	36.30	17.69	18.61
La	1.78	0.05	0.24	2.00	0.90	1.10
Ni	7.91	0.70	3.45	12.28	-1.74	14.02
PbLa1	21.27	5.94	29.12	151.01	2.62	148.40
PbLb1	12.35	1.38	6.76	30.51	-0.74	31.25
Sr	3.76	0.19	0.95	5.68	1.99	3.69
Zn	35.35	3.96	19.40	102.99	7.18	95.82
Zr	18.40	0.17	0.83	20.82	17.33	3.48

Table 6 **Cataract**

	Mean	SE	SD	Maximum	Minimum	Range
Elements						
Ba	11.17	0.34	1.97	15.46	7.84	7.62
Co	1.90	0.06	0.36	2.73	1.34	1.39
Cr	31.56	1.35	7.76	51.42	19.64	31.78
La	1.80	0.04	0.24	2.00	0.88	1.12
Ni	8.73	0.42	2.39	12.58	3.51	9.07
PbLa1	2.92	0.10	0.55	5.51	2.62	2.90
PbLb1	-1.21	0.54	3.10	4.40	-7.43	11.83
Sr	4.95	0.18	1.02	7.23	2.69	4.54
Zn	6.59	0.44	2.52	15.56	2.80	12.76
Zr	19.44	0.28	1.61	25.96	17.89	8.07

Table 7 **HIXTON**

	Mean	SE	SD	Maximum	Minimum	Range
Elements						
Ba	12.63	0.53	3.06	21.07	8.01	13.06
Co	2.14	0.11	0.61	4.84	1.20	3.64
Cr	27.81	1.42	8.18	52.05	17.76	34.30
La	1.83	0.03	0.17	2.00	1.35	0.65
Ni	7.21	0.74	4.24	17.02	-4.86	12.16
PbLa1	3.56	0.22	1.24	8.61	2.62	5.99
PbLb1	0.11	0.58	3.32	6.67	-5.90	12.58
Sr	4.97	0.20	1.17	7.96	3.39	4.57
Zn	6.37	0.60	3.43	15.37	2.50	12.87
Zr	20.12	0.31	1.75	26.03	18.49	7.53

DISCUSSION/CONCLUSION

In summary, I have argued that the sourcing of silicified sandstones in the UMRV should be done more objectively, using quantifiable data, and avoid using physical traits and characteristics such as color, texture, or grain size. I argue that pXRF analysis, aided by calibration and quantification standards provided by ICP-MS data is a suitable alternative to macroscopic sourcing techniques.

I have identified four elements (Pb, Sr, Zn, and Zr) from my analysis, for which pXRF can produce reliable calibrated and quantified results, making these elements suitable for pXRF analysis of silicified sandstones. In addition, I have also demonstrated that several elements (Ba, Co, Cr, La, and Ni), within the detection limits for both pXRF and ICP-MS, produce unreliable pXRF results compared to ICP-MS analysis results, making these elements unsuitable for pXRF

analysis of silicified sandstones. Thus, pXRF analysis, aided by calibration and quantification standards provided by ICP-MS data, of lead (Pb), strontium (Sr), zinc (Zn), and zirconium (Zr) produces reliable results, which can then be compared to help differentiate between silicified sandstones in the UMRV.

In addition, I have demonstrated that Arcadia Ridge, Cataract, and Hixton silicified sandstones can be differentiated, at the formation level, by analyzing the amounts of lead and zinc within a given sample. Arcadia Ridge silicified sandstone has been demonstrated to have higher lead (calculated from the PbLa1 energy level) and zinc mean values than Hixton and Cataract silicified sandstones. Meaning that higher lead and zinc values, from pXRF analysis is likely indicative of Arcadia Ridge silicified sandstone, which belongs to the Jordan formation. Conversely, relatively low lead and zinc values are indicative of Cataract and Hixton silicified sandstones, both of which belong to the Wonewoc formation. However, this study also found that pXRF does not have the precision to differentiate at the formation level, specifically between Cataract and Hixton silicified sandstone. Future studies can be directed at determining if any other form of geochemical analysis is useful in differentiating UMRV silicified sandstones at the formation level. This would increase the depth of our understanding of pre-historic use of silicified sandstone in the UMRV by being able to source silicified sandstone artifacts to the source level.

I have also shown that pXRF analysis of the cortex of silicified sandstones is inaccurate due to that part of the stone being elementally different than the rest of the stone. Now in future pXRF studies of artifacts can, and should, avoid scanning cortex areas, or areas in close proximity to cortex as these will result in “un-uniform” results compared to the rest of the tool-stone.

The results of this study has implications for the field of archaeology and those interested in the geochemical sourcing of sandstones in the UMRV from archaeological sites. First, the calibration and quantification standards developed from the ICP-MS data attained could be applied to silicified sandstones attained from sites in the area and be used to produce calibrated, quantified pXRF results. These results can then be used to elementally characterize each sample, which will help determine which source, or formation, each sample best conforms to. After determining lithic source and material preferences at sites a suite of human behaviors based on materials present at the sites, the sites location, and the geographic positioning of the lithic sources, and the relation between those three factors. These human behaviors include population movements, exchange/trade networks, and access to/or lack of access to lithic sources. For example, Paleo-Indian assemblages, which have a fairly high occurrence of silicified sandstone (Lang 1987:132; Boszhardt and Carr 2010:19; Mason 1988: 28), can be geochemically sourced using standards and methods developed during this study. The geochemical sourcing of Paleo-Indian assemblages containing these silicified sandstones could help shed light on social behaviors such as Paleo-Indian mobility or landscape usage. However, results from this study could also be applied to any site, dating to any time period, so long as it contains silicified sandstones for which data has been accumulated. In summary, pXRF analysis, combined with calibration and quantification standards developed through ICP-MS analysis offers the archaeologist a quantifiable, non-destructive method for sourcing silicified sandstones, which in turn can lead to the discussion of a range of social behavior relating to how people use and relate to their geophysical and social landscape.

Appendix 1. All ICP-MS values by sample

Elements	Ba	Ce	Cr	Cs	Dy	Er	Eu	Ga	Gd	Hf	Ho	La	Lu	Nb	Nd	Pr	Rb	Sm	Sn	Sr
Samples	ppm	ppm	ppm	ppm	ppm	ppm	ppm	ppm	ppm	ppm	ppm	ppm	ppm	ppm	ppm	ppm	ppm	ppm	ppm	ppm
SM-SA1-S-2	15.3	4.3	40	0.04	0.17	0.07	0.04	1	0.23	0.6	0.03	2.8	0.02	0.3	1.5	0.46	1.1	0.24	1	5.9
SM-SA2-S-5	9.7	2.4	50	0.05	0.17	0.09	0.05	0.9	0.18	0.6	0.04	1.5	0.02	0.3	0.9	0.24	1.2	0.22	1	5.1
SM-SA3-S-7	4.2	3.6	10	0.04	0.19	0.1	0.03	0.4	0.17	0.6	0.03	2.2	0.02	0.2	1.2	0.33	0.4	0.22	<1	4.3
SM-SA5-10	12	4.4	20	0.06	0.21	0.12	0.03	0.6	0.23	0.6	0.04	2.8	0.02	0.3	1.4	0.39	1	0.28	1	6.2
SM-SA4-S-8	4.8	2.9	30	0.03	0.17	0.12	0.04	0.7	0.19	0.6	0.03	1.9	0.02	0.2	1	0.26	0.3	0.19	<1	3.9
SM-SA5-S-11	14.8	6.5	50	0.05	0.2	0.09	0.06	1.4	0.16	0.5	0.03	4.2	0.03	0.3	2	0.58	1.3	0.34	1	9.6
AR-SA1-S-1-F-2	8.3	2.8	20	0.04	0.15	0.08	0.03	0.7	0.17	0.4	0.03	1.2	0.02	0.2	1.1	0.28	0.5	0.19	<1	2.6
AR-SA2-S-2	8.3	3.1	10	0.06	0.18	0.06	0.06	0.3	0.25	0.5	0.04	1.3	0.02	<0.2	1.3	0.3	0.5	0.24	<1	2.7
AR-SA2-S-4	8.7	3.3	20	0.03	0.23	0.08	0.05	0.4	0.18	0.5	0.03	1.3	0.03	<0.2	1.3	0.31	0.4	0.24	<1	2.3
AR-SA2-S-5	9.7	3.3	20	0.05	0.17	0.06	0.04	0.5	0.24	0.4	0.03	1.5	0.01	0.2	1.3	0.35	0.4	0.27	<1	2.7
AR-SA3-S-7	10.3	3.4	40	0.05	0.22	0.09	0.05	0.9	0.2	0.5	0.04	1.5	0.03	<0.2	1.4	0.33	0.6	0.21	<1	3.2
Cat.-S-1	77	3.5	10	0.04	0.2	0.1	0.06	0.7	0.18	0.4	0.04	2	0.02	0.3	1.5	0.38	0.4	0.28	<1	7.9
Cat.-S-2	7.9	3.1	70	0.03	0.15	0.08	0.03	1.9	0.21	0.5	0.03	2.1	0.02	0.4	1	0.32	0.3	0.23	<1	3.9
Cat.-S-5	11.1	3.5	30	0.06	0.14	0.07	0.03	0.9	0.14	0.5	0.01	1.4	0.01	0.2	1.3	0.33	0.8	0.17	<1	2.2
Cat.-S-7	9.8	2.6	40	0.03	0.2	0.12	0.03	1.1	0.17	0.6	0.04	1.7	0.02	0.3	1	0.3	0.4	0.22	<1	7.2
Cat.-S-8	7.4	3.1	40	0.03	0.16	0.09	0.04	1.2	0.21	0.5	0.04	1.8	0.02	0.2	1.3	0.34	0.5	0.22	1	4.6

Appendix 1. Continued

Elements	Ta	Tb	Th	Tm	U	V	W	Y	Yb	Zr		SiO2	Al2O3	Fe2O3	CaO	MgO	Na2O	K2O	Cr2O3	TiO2
Samples	ppm	ppm	ppm	ppm	ppm	ppm	ppm	ppm	ppm	ppm		%	%	%	%	%	%	%	%	%
SM-SA1-S-2	<0.1	0.02	0.42	0.03	0.22	<5	<1	1	0.13	21	/	95.7	0.11	6.47	0.04	0.02	0.02	0.04	<0.01	0.01
SM-SA2-S-5	<0.1	0.03	0.42	0.02	0.19	<5	<1	1	0.1	24	/	94.2	0.16	9.22	0.06	0.03	0.01	0.03	0.01	0.01
SM-SA3-S-7	<0.1	0.02	0.42	0.01	0.2	<5	<1	0.9	0.11	21	/	99.9	0.04	2.17	0.01	<0.01	<0.01	0.02	<0.01	0.01
SM-SA5-10	<0.1	0.02	0.47	0.02	0.24	<5	<1	1.2	0.15	26	/	95.8	0.13	5.32	0.04	0.01	0.02	0.03	<0.01	0.01
SM-SA4-S-8	<0.1	0.03	0.4	0.02	0.19	<5	<1	1	0.13	24	/	97	0.07	4.51	0.01	0.01	<0.01	0.01	<0.01	0.01
SM-SA5-S-11	<0.1	0.04	0.38	0.01	0.16	<5	<1	1.1	0.1	21	/	92.2	0.15	11	0.04	0.02	<0.01	0.04	0.01	0.02
AR-SA1-S-1-F-2	<0.1	0.02	0.43	0.01	0.34	<5	<1	1	0.11	15	/	96.4	0.07	6.36	0.05	0.01	0.01	0.02	<0.01	0.01
AR-SA2-S-2	<0.1	0.03	0.47	0.02	0.59	<5	<1	1	0.1	16	/	99.4	0.07	2.55	0.03	0.01	0.01	0.02	<0.01	0.01
AR-SA2-S-4	<0.1	0.03	0.47	0.02	0.6	<5	<1	1.1	0.12	17	/	95.2	0.08	3	0.04	0.01	<0.01	0.02	<0.01	0.01
AR-SA2-S-5	<0.1	0.03	0.57	0.02	0.6	<5	<1	0.9	0.08	14	/	97.5	0.06	4.45	0.03	0.01	<0.01	0.02	<0.01	0.01
AR-SA3-S-7	<0.1	0.03	0.49	0.02	2.92	<5	<1	1.2	0.12	18	/	93.9	0.08	7.43	0.17	0.02	0.01	0.02	0.01	0.01
Cat.-S-1	<0.1	0.02	0.52	0.01	0.21	<5	<1	0.9	0.08	19	/	99.3	0.05	2.05	0.03	0.01	<0.01	0.02	<0.01	0.01
Cat.-S-2	<0.1	0.03	0.42	0.02	0.16	<5	<1	1	0.09	19	/	88.9	0.08	16.3	0.02	0.01	0.01	0.01	0.01	0.01
Cat.-S-5	<0.1	0.02	0.44	0.01	0.39	<5	<1	0.8	0.07	17	/	95.5	0.1	5.74	0.02	0.01	0.01	0.04	<0.01	0.01
Cat.-S-7	<0.1	0.02	0.32	0.02	0.19	<5	<1	0.9	0.14	21	/	95.2	0.07	8.05	0.02	0.01	<0.01	0.02	0.01	0.01
Cat.-S-8	<0.1	0.02	0.37	0.01	0.21	<5	1	0.9	0.11	19	/	91.3	0.1	10.7	0.03	0.01	0.01	0.03	0.01	0.01

Appendix 1. Continued

Elements	MnO	P2O5	SrO	BaO	LOI	Total		Ag	As	Cd	Co	Li	Mo	Ni	Pb	Sc	Tl	Zn
Samples	%	%	%	%	%	%		ppm	ppm	ppm	ppm	ppm	ppm	ppm	ppm	ppm	ppm	ppm
SM-SA1-S-2	0.06	<0.01	<0.01	<0.01	-1.36	101.11	`	<0.5	<5	<0.5	3	<10	1	7	4	<1	<10	7
SM-SA2-S-5	0.09	0.01	<0.01	<0.01	-2.08	101.75	`	<0.5	<5	<0.5	2	<10	1	12	<2	<1	<10	4
SM-SA3-S-7	0.02	<0.01	<0.01	<0.01	-0.3	101.87	`	<0.5	<5	<0.5	1	<10	1	5	<2	<1	<10	<2
SM-SA5-10	0.05	0.01	<0.01	<0.01	-1.29	100.13	`	<0.5	<5	<0.5	2	<10	1	7	<2	<1	<10	2
SM-SA4-S-8	0.04	0.01	<0.01	<0.01	-0.71	100.96	`	<0.5	<5	<0.5	2	<10	1	7	<2	<1	<10	2
SM-SA5-S-11	0.1	0.01	<0.01	<0.01	-2.56	101.03	`	<0.5	<5	<0.5	2	<10	2	15	<2	<1	<10	9
AR-SA1-S-1-F-2	0.06	0.01	<0.01	<0.01	-1.24	101.76	`	<0.5	<5	<0.5	2	<10	2	13	23	<1	<10	47
AR-SA2-S-2	0.02	<0.01	<0.01	<0.01	-0.3	101.82	`	<0.5	<5	<0.5	1	<10	1	4	13	<1	<10	56
AR-SA2-S-4	0.03	<0.01	<0.01	<0.01	-0.2	98.19	`	<0.5	<5	<0.5	1	<10	<1	5	10	<1	<10	44
AR-SA2-S-5	0.04	0.01	<0.01	<0.01	-0.98	101.15	`	<0.5	<5	<0.5	2	<10	2	12	11	<1	<10	52
AR-SA3-S-7	0.07	0.01	<0.01	<0.01	-1.19	100.54	`	<0.5	<5	<0.5	2	<10	1	12	2	1	<10	20
Cat.-S-1	0.02	<0.01	<0.01	0.01	-0.06	101.44	`	<0.5	<5	<0.5	1	<10	1	4	<2	<1	<10	3
Cat.-S-2	0.15	0.01	<0.01	<0.01	-5.26	100.25	`	<0.5	<5	<0.5	5	<10	5	27	<2	<1	<10	2
Cat.-S-5	0.06	<0.01	<0.01	<0.01	-1.13	100.36	`	<0.5	<5	<0.5	1	<10	1	11	<2	<1	<10	7
Cat.-S-7	0.07	<0.01	<0.01	<0.01	-1.68	101.78	`	<0.5	<5	<0.5	3	<10	2	14	<2	<1	<10	3
Cat.-S-8	0.1	0.01	<0.01	<0.01	-2.33	99.98	`	<0.5	<5	<0.5	3	<10	2	13	2	<1	<10	4

Appendix 2: ICP-MS values deemed useful to this study

Elements	Ba	Cr	La	Rb	Sr	Zr	Co	Ni	Pb	Zn
Samples	ppm	ppm	ppm	ppm	ppm	ppm	ppm	ppm	ppm	ppm
SM-SA1-S-2	15.3	40	2.8	1.1	5.9	21	3	7	4	7
SM-SA2-S-5	9.7	50	1.5	1.2	5.1	24	2	12	<2	4
SM-SA3-S-7	4.2	10	2.2	0.4	4.3	21	1	5	<2	<2
SM-SA5-10	12	20	2.8	1	6.2	26	2	7	<2	2
SM-SA4-S-8	4.8	30	1.9	0.3	3.9	24	2	7	<2	2
SM-SA5-S-11	14.8	50	4.2	1.3	9.6	21	2	15	<2	9
AR-SA1-S-1-F-2	8.3	20	1.2	0.5	2.6	15	2	13	23	47
AR-SA2-S-2	8.3	10	1.3	0.5	2.7	16	1	4	13	56
AR-SA2-S-4	8.7	20	1.3	0.4	2.3	17	1	5	10	44
AR-SA2-S-5	9.7	20	1.5	0.4	2.7	14	2	12	11	52
AR-SA3-S-7	10.3	40	1.5	0.6	3.2	18	2	12	2	20
Cat.-S-1	77	10	2	0.4	7.9	19	1	4	<2	3
Cat.-S-2	7.9	70	2.1	0.3	3.9	19	5	27	<2	2
Cat.-S-5	11.1	30	1.4	0.8	2.2	17	1	11	<2	7
Cat.-S-7	9.8	40	1.7	0.4	7.2	21	3	14	<2	3
Cat.-S-8	7.4	40	1.8	0.5	4.6	19	3	13	2	4

Appendix 4. All calibrated pXRF values

Samples	**Elements**									
	BaLa1	**LaLa1**	**CrKa1**	**CoKa1**	**NiKa1**	**ZnKa1**	**PbLa1**	**PbLb1**	**SrKa1**	**ZrKa1**
AR-hwy93-sample area 1-sample-1-f-1-scan-1-gf	12.79	1.35	29.84	1.26	7.01	24.99	23.97	18.09	1.99	18.71
AR-hwy93-sample area 1-sample-1-f-1-scan-2-gf	13.64	1.99	29.07	1.16	5.72	20.78	21.41	13.83	3.65	17.59
AR-hwy93-sample area 1-sample-1-f-1-scan-3-gf	10.33	1.94	26.99	1.13	11.10	24.93	26.68	12.58	4.19	18.04
AR-hwy93-sample area 1-sample-1-f-2-scan-1-gf	10.04	1.96	17.69	2.01	11.09	47.15	23.25	23.21	4.56	20.36
AR-hwy93-sample area 1-sample-1-f-2-scan-2-gf	16.25	1.98	18.34	6.61	5.69	66.01	40.89	18.11	5.07	19.01
AR-hwy93-sample area 1-sample-1-f-2-scan-3-gf	11.20	1.80	18.27	50.92	5.06	102.99	151.01	30.51	4.40	20.82
AR-hwy93-sample area 2-sample-2-scan-1-gf	8.54	1.83	24.31	1.04	6.26	28.92	12.53	11.04	2.60	18.33
AR-hwy93-sample area 2-sample-2-scan-2-gf	14.18	1.81	32.14	1.26	8.66	41.21	15.35	11.68	2.52	18.70
AR-hwy93-sample area 2-sample-2-scan-3-gf	9.92	1.68	20.91	1.08	-1.74	36.09	5.03	14.34	3.12	17.89
AR-hwy93-sample area 2-sample-3-scan-1-gf	11.32	2.00	24.25	1.09	10.60	34.58	22.83	15.71	5.68	19.02
AR-hwy93-sample area 2-sample-3-scan-2-gf	15.78	1.99	21.37	1.12	6.87	30.99	20.38	12.50	4.21	17.85
AR-hwy93-sample area 2-sample-3-scan-3-gf	11.70	1.78	32.33	1.04	6.27	39.88	8.86	10.90	4.03	18.06
AR-hwy93-sample area 2-sample-4-scan-1-gf	19.00	1.74	24.98	1.04	3.09	32.32	22.02	14.01	5.34	17.93
AR-hwy93-sample area 2-sample-4-scan-2-gf	14.06	1.77	33.78	1.05	8.97	48.83	22.67	10.45	4.83	17.52
AR-hwy93-sample area 2-sample-4-scan-3-gf	12.85	1.84	28.61	1.51	2.30	31.15	19.82	12.08	3.92	18.48
AR-hwy93-sample area 2-sample-5-scan-1-gf	17.09	1.88	26.12	1.33	10.60	36.72	10.55	17.54	2.94	17.33
AR-hwy93-sample area 2-sample-5-scan-2-gf	9.17	1.60	27.21	1.19	10.35	35.26	6.92	10.30	3.79	18.74
AR-hwy93-sample area 2-sample-5-scan-3-gf	11.93	1.85	28.26	1.17	10.38	37.98	6.92	10.45	3.63	18.61
AR-hwy93-sample area 2-sample-6-scan-1-gf	11.64	1.67	31.42	1.24	8.81	29.04	13.47	8.40	3.68	18.24
AR-hwy93-sample area 2-sample-6-scan-2-gf	7.54	1.78	36.30	1.48	9.07	43.87	14.16	10.45	2.55	18.18
AR-hwy93-sample area 2-sample-6-scan-3-gf	11.26	0.90	35.31	1.61	7.69	27.18	12.49	9.66	3.22	17.90
AR-hwy93-sample area 3-sample-7-scan-1-gf	9.33	1.77	28.78	2.15	11.97	8.61	2.62	1.08	4.07	17.74
AR-hwy93-sample area 3-sample-7-scan-2-gf	10.62	2.00	32.64	2.30	12.28	11.86	3.92	-0.74	2.78	18.71
AR-hwy93-sample area 3-sample-7-scan-3-gf	7.97	1.91	21.77	2.55	11.75	7.18	2.65	0.11	3.53	17.74
cataract-s.s.-sample-1-scan-2-gf	11.38	1.96	19.64	1.54	5.60	8.89	3.62	1.18	6.29	19.91
cataract-s.s.-sample-1-scan-1-gf	9.98	1.70	23.85	1.36	10.06	6.73	2.62	2.84	6.06	18.04

cataract-s.s.-sample-1-scan-3-g.f	12.97	1.61	29.29	1.38	7.23	7.72	2.70	-3.30	6.12	20.26
Appendix 4. Continued	**BaLa1**	**LaLa1**	**CrKa1**	**CoKa1**	**NiKa1**	**ZnKa1**	**PbLa1**	**PbLb1**	**SrKa1**	**ZrKa1**
cataract-s.s.-sample-2-scan-1-gf	8.68	1.89	31.69	1.91	7.18	7.78	2.62	-1.62	4.30	19.87
Cataract-ss-sample-2-scan-3-g.f	12.76	1.97	26.88	2.16	8.17	4.77	2.63	-5.74	4.44	19.18
cataract-s.s.-sample-2-scan-2-gf	8.93	1.57	40.27	1.60	4.94	4.54	2.72	-3.54	3.40	19.53
cataract-s.s.-sample-3-scan-1-gf	15.46	1.95	27.85	1.62	3.51	10.32	3.48	4.11	4.94	19.17
cataract-s.s.-sample-3-scan-2-gf	11.24	1.77	40.62	1.38	11.60	5.35	3.38	-0.59	4.16	18.11
cataract-ss-sample-3-scan-3-g.f	13.91	1.87	24.55	1.34	7.98	7.02	2.62	0.84	5.02	18.63
cataract-s.s.-sample-4-scan-1-gf	10.71	1.92	25.49	1.61	9.37	4.78	2.69	-1.25	6.04	18.95
cataract-s.s.-sample-4-scan-2-gf	8.20	1.14	31.74	1.92	11.27	7.59	2.84	-1.03	5.51	19.17
cataract-ss-sample-4-scan-3-g.f	7.84	1.89	49.95	1.57	12.58	9.83	2.82	1.72	5.77	18.28
cataract-s.s.-sample-5-scan-1-gf	13.03	1.98	35.08	1.71	11.09	6.77	3.35	2.28	2.69	18.74
cataract-s.s.-sample-5-scan-2-gf	11.72	1.66	34.52	1.98	8.28	15.56	2.62	3.35	4.03	18.32
cataract-ss-sample-5-scan-3-g.f	13.20	2.00	23.78	1.59	11.11	7.00	2.85	-0.59	3.29	19.47
cataract-s.s.-sample-6-scan-1-gf	10.42	1.49	20.37	1.81	11.72	4.99	5.51	-4.00	5.78	18.79
cataract-s.s.-sample-6-scan-2-gf	8.42	0.88	35.86	1.83	9.77	6.82	2.68	-2.93	4.84	18.53
Cataract-ss-sample-6-scan-3-g.f	9.97	1.86	31.12	2.22	6.88	9.70	2.65	-1.37	5.45	23.18
cataract-s.s.-sample-7-scan-1-gf	9.88	1.83	43.13	2.51	8.67	2.80	2.64	-4.31	7.23	20.50
cataract-s.s.-sample-7-scan-2-gf	13.69	1.91	28.09	2.35	3.83	2.94	3.47	-1.55	5.99	19.61
cataract-ss-sample-7-scan-3-g.f	11.30	1.94	36.89	2.06	8.02	7.79	2.91	0.23	6.57	21.75
cataract-s.s.-sample-8-scan-1-gf	9.13	1.85	51.42	2.12	9.13	5.58	2.65	-4.50	4.31	17.89
cataract-s.s.-sample-8-scan-2-gf	10.27	1.79	28.39	1.90	11.14	5.25	2.62	-1.59	4.54	18.72
Cataract-ss-sample-8-scan-3-g.f	9.96	1.85	34.31	1.60	8.83	6.18	2.63	-6.63	4.51	18.92
cataract-s.s.-sample-9-scan-1-gf	12.35	1.78	31.65	1.96	9.48	3.46	2.82	-4.48	4.87	20.75
cataract-s.s.-sample-9-scan-2-gf	12.85	1.99	26.40	2.73	5.18	5.47	3.12	-3.52	4.18	18.35
cataract-s.s.-sample-9-scan-3-gf	13.86	1.92	21.22	2.43	9.97	6.13	2.82	-0.29	5.35	18.55
cataract-s.s.-sample-10-scan-2-gf	11.14	1.95	32.00	1.78	6.25	7.34	2.67	4.40	4.86	18.19
cataract-ss-sample-10-scan-3-g.f	11.76	1.82	26.08	2.38	10.75	4.43	3.02	-7.43	4.40	18.36
cataract-s.s.-sample-11-scan-2-gf	9.66	1.97	32.66	1.97	8.74	6.61	2.70	-0.42	3.87	19.11
cataract-ss-sample-11-scan-3-g.f	14.15	2.00	28.89	1.97	8.85	6.07	2.72	3.50	3.83	19.51

cataract-s.s.-sample-12-scan-2-gf	9.05	1.72	41.17	2.32	12.38	8.30	2.62	-0.03	5.36	25.96
Appendix 4. Continued	**BaLa1**	**LaLa1**	**CrKa1**	**CoKa1**	**NiKa1**	**ZnKa1**	**PbLa1**	**PbLb1**	**SrKa1**	**ZrKa1**
cataract-ss-sample-12-scan-3-g.f	10.76	1.92	26.67	1.98	8.53	2.95	2.62	-3.49	5.33	19.15
hixton-11-11-15-sample-area-1-sample-1-scan-1-gf	13.61	1.75	19.08	1.88	10.60	5.40	2.72	-4.55	4.68	18.90
hixton-11-11-15-sample-area-1-sample-1-scan-2-gf	11.98	1.84	32.28	4.84	6.45	15.23	2.69	-4.39	3.82	19.50
hixton-11-11-15-sample-area-1-sample-1-scan-3-gf	9.39	1.98	17.76	1.98	10.68	7.60	2.84	2.92	4.70	19.05
hixton-11-11-15-sample-area-1-sample-2-scan-1-gf	12.98	1.99	23.64	2.31	6.97	5.60	3.61	6.67	5.99	20.08
hixton-11-11-15-sample-area-1-sample-2-scan-2-gf	14.30	1.78	21.13	2.01	12.16	7.19	3.90	0.03	4.97	19.52
hixton-11-11-15-sample-area-1-sample-2-scan-3-gf	15.66	1.75	21.09	2.26	3.85	3.82	8.61	3.02	5.49	19.71
hixton-11-11-15-sample-area-1-sample-3-scan-1-gf	11.81	1.87	24.00	2.05	10.99	6.07	2.92	0.30	4.36	20.82
hixton-11-11-15-sample-area-1-sample-3-scan-2-gf	16.91	1.96	21.61	1.20	9.26	3.57	2.68	-5.90	4.39	20.43
hixton-11-11-15-sample-area-1-sample-3-scan-3-gf	9.87	1.99	32.11	1.64	8.70	6.78	3.87	-4.88	4.15	20.43
hixton-11-11-15-sample-area-2-sample-4-scan-1-gf	12.68	2.00	21.54	1.85	9.05	4.31	3.24	-3.11	5.24	19.57
hixton-11-11-15-sample-area-2-sample-4-scan-2-gf	11.17	1.97	25.39	2.20	10.72	4.45	2.65	-0.06	5.05	19.35
hixton-11-11-15-sample-area-2-sample-4-scan-3-gf	21.07	1.84	19.91	2.02	5.38	4.82	5.17	1.53	5.19	19.07
hixton-11-11-15-sample-area-2-sample-5-scan-1-gf	10.67	1.35	33.04	2.64	11.77	2.59	3.13	-3.79	3.61	20.27
hixton-11-11-15-sample-area-2-sample-5-scan-2-gf	8.86	2.00	30.51	2.11	8.72	3.54	2.70	0.10	3.55	19.65
hixton-11-11-15-sample-area-2-sample-5-scan-3-gf	9.25	1.56	29.55	1.93	8.17	5.39	3.75	-3.77	4.01	19.56
hixton-11-11-15-sample-area-2-sample-6-scan-1-gf	8.43	1.98	36.27	2.51	8.92	8.10	2.62	1.49	6.76	18.96
hixton-11-11-15-sample-area-2-sample-6-scan-2-gf	11.18	1.75	31.51	1.52	9.32	4.30	4.71	-5.85	5.86	19.32
hixton-11-11-15-sample-area-2-sample-6-scan-3-gf	15.77	2.00	34.48	1.93	7.80	4.78	2.64	2.66	5.59	18.50
hixton-11-11-15-sample-area-3-sample-7-scan-1-gf	14.23	1.82	34.73	2.37	4.61	6.87	3.50	4.58	4.48	22.25
hixton-11-11-15-sample-area-3-sample-7-scan-2-gf	16.85	2.00	22.23	2.25	4.97	4.72	4.92	-0.60	3.50	18.53
hixton-11-11-15-sample-area-3-sample-7-scan-3-gf	17.60	1.91	18.17	2.02	-4.86	5.04	5.96	3.21	5.13	19.75
hixton-11-11-15-sample-area-4-sample-8-scan-1-gf	11.53	1.66	28.61	2.14	8.95	3.80	2.92	-0.47	4.06	20.21
hixton-11-11-15-sample-area-4-sample-8-scan-2-gf	9.47	1.81	36.45	2.62	10.87	2.99	3.49	0.57	3.39	21.53
hixton-11-11-15-sample-area-4-sample-8-scan-3-gf	11.36	1.92	21.42	2.49	7.78	5.97	2.66	-1.37	3.74	25.83
hixton-11-11-15-sample-area-4-sample-9-scan-1-gf	11.65	1.90	24.71	1.69	7.17	5.72	3.13	-0.90	5.27	19.61
hixton-11-11-15-sample-area-4-sample-9-scan-2-gf	13.28	1.69	17.98	2.25	-3.49	15.37	4.26	3.73	4.07	18.49
hixton-11-11-15-sample-area-4-sample-9-scan-3-gf	12.72	1.90	22.85	2.84	10.82	8.05	3.26	0.46	5.47	19.05

Appendix 4. Continued	**BaLa1**	**LaLa1**	**CrKa1**	**CoKa1**	**NiKa1**	**ZnKa1**	**PbLa1**	**PbLb1**	**SrKa1**	**ZrKa1**
hixton-11-11-15-sample-area-5-sample-10-scan-1-gf	9.55	2.00	30.49	1.29	6.13	6.97	2.98	-1.65	5.92	26.03
hixton-11-11-15-sample-area-5-sample-10-scan-2-gf	13.28	1.69	17.98	2.25	-3.49	15.37	4.26	3.73	4.07	18.49
hixton-11-11-15-sample-area-5-sample-10-scan-3-gf	17.35	1.97	37.76	1.45	3.24	2.50	2.66	3.46	5.08	21.85
hixton-11-11-15-sample-area-5-sample-11-scan-1-gf	13.26	1.72	34.02	1.91	9.91	6.01	3.55	0.94	7.36	20.30
hixton-11-11-15-sample-area-5-sample-11-scan-2-gf	8.01	1.77	52.05	2.03	8.97	5.28	2.64	5.53	7.28	19.93
hixton-11-11-15-sample-area-5-sample-11-scan-3-gf	10.95	1.40	43.39	2.06	6.72	11.93	2.76	0.01	7.96	19.24

References Cited

Andrefsky, William Jr.

2005 *Lithics; Macroscopic Approaches to Analysis.* Cambridge University Press 2nd Edition.

Boszhardt, Robert

1998 An Archeological Survey of an Othroquartzite District in West-Central Wisconsin. *Reports of Investigations No. 306.* Mississippi Valley Archaeology Center, University of Wisconsin La Crosse.

2003 *A Projectile Point Guide for the Upper Mississippi River Valley.* University of Iowa Press, Iowa City

2012 An Archaeological Reconnaissance of New Rockshelters and Silicified Sandstone Sources in Trempealeau and Buffalo Counties, Wisconsin. *Wisconsin Archaeological Society*

Boszhardt, Robert and Dillion Carr

2010 Silver Mound, Wisconsin: Source of Hixton Silicified Sandstone. *Midcontinental Journal of Archaeology* 35(1): pp. 5–36.

Drake, Lee

2014 XRF Guru: pXRF User Guide. www.xrf.guru

Golitko, Mark, James Meirhoff, and John Edward Terrell

2010 Chemical characterization of sources of obsidian from the Sepik coast *Archaeology in Oceania* 45(3):pp.120-129

Hill, Matthew Glenn

1994 Paleoindian Projectile Points From the Vicinity of Silver Mound (47Ja21), Jackson County, Wisconsin. *Midcontinental Journal of Archaeology* 19(2) pp. 223-259

Juling et al.

2002 Provenance Studies of Late Paleo-Indian Quartzite Artifacts in the Great Lakes Region Using Destructive and Non-Destructive Techniques. *Archaeolingua.* Centeral European Series 1, Archaeometry 98

Lang, James

2004 Wisconsin Prehistoric Lithic Materials *Central States Archaeological Journal* 51(4) pp. 104-111

Lang, James

1987 Hixton Silicified Sandstone: Wisconsin's Unique Prehistoric Lithic Material. *Central States Archaeological Journal.* 34(3): pp. 131-141.

Mason, Carol

1988 *Introduction to Wisconsin Indians: Prehistory to Statehood.* Sheffield Publishing, Salem Wisconsin.

Mossler, John

2008 Paleozoic Stratigraphic Nomenclature for Minnesota. *Report of Investigations 65.* University of Minnesota

Nazaroff et al.

2010 Assessing the Applicability of Portable X-ray Fuorescence Spectrometry for Obsidian Provenance Research in the Maya Lowlands. *Journal of Archaeological Science.* 37: pp. 885–895

Ostrum, Meredith

1973 Guidebook to the Geology and Mineral Deposits of the Centeral Part of Jackson County and Part of Clark County, Wisconsin. *Wisconsin Geological and Natural History Surveys.*

Pauketet, Timothy

2004 *Ancient Cahokia and the Mississippians*. Cambridge University Press. UK.

Porter, James

1961 Hixton Silicified Sandstone: a Unique Lithic Material Used by Prehistoric Cultures. *Wisconsin Archaeologist* 42(2): pp. 78-85.

Price, Douglas and James Burton

2011 *An Introduction to Archaeological Chemistry* Springer Press NY

Runkel, Tony

2012 Goodhue County Bedrock Geology: Relevance to Silica Sand Mining *Minnesota Geologic Survey*

Runkel et al.

2012 Conference on the Silica Sand Resources of Minnesota and Wisconsin: Field-Guide Book. *Minnesota Geologic Survey.* PRC Guidebook 12-01

Smith et al.

2007 Sources of Imported Obsidian at Postclassic Sites in the Yautepec Valley, Morelos: A Characterization Study Using XRF and INAA. *Latin American Antiquity*,18(4): pp. 429-450

Weldon, K.

2010 The Hotter Side of Obsidian. Oregon State University. volcano.oregonstate.edu/obsidian-formation.

Wendt Dan

2015 Physical Attribute Guide to the Minnesota Historical Society Lithic Comparative Collection. Minnesota Historical Society